PROLONGATION OF THE DEPLOYMENT AND MONITORING OF A MULTIPLE OSCILLATING WATER COLUMN WAVE ENERGY CONVERTER

V/06/00190/REP

URN 03/634

Contractor

The University of Plymouth.
Department of Mechanical and Marine Engineering

Authors

Mr F.Johnson
Dr J.Chudley
Dr Y.M.Dai

The work described in this report was carried out under contract as part of the DTI New and Renewable Energy Programme. The views and judgements expressed in this report are those of the contractor and do not necessarily reflect those of the DTI.

First Published 2003

EXECUTIVE SUMMARY

Introduction

The Department of Trade and Industry (DTI) contracted the University of Plymouth to prolong the deployment of its prototype Multiple Oscillating Water Column (MOWC) wave energy device. The prolongation of the sea trials period allowed the generation of physical data from which an evaluation of the concept and an estimation of the overall conversion efficiency achieved during the sea trials period could be calculated.

This report gives a brief background to the origins of the prototype device and presents the methodology for the analysis of the prototype conversion efficiency, calculated for the period of the sea trials as ***34.5%.***

Project aims and objectives

Evaluation of the prototype wave energy device was conducted with the following aims and objectives.

The aims of the project were:

(i) to complete a full analysis of the sea trials data with regard to the incident wave power and power generated across the turbine;

(ii) to evaluate the MOWC concept with regard to the conversion efficiency;

(iii) to recommend future areas of research and development that would increase the conversion efficiency of the concept design;

(iv) to present the physical data into the public domain on a web based site;

In order to complete these aims the objectives of the project were as follows:

(i) the continued deployment of the prototype MOWC prototype for a further period of 12 months;

(ii) the evaluation of the MOWC concept in its ability to generate a stable and reliable power for the production of electricity within predefined limits;

(iii) to recommend improvements that could be made to the prototype design in order to increase the conversion efficiency;

Background

The integration of a renewable energy generator into an electrical distribution grid requires the flow of electricity to be maintained within specific limits of voltage and cycles. The

ability of a renewable energy system to generate a stable and reliable flow of electricity is therefore of paramount importance to its commercial success.

Within the MOWC prototype, individual oscillating columns were ducted to exhaust into and extract air from a single self-rectifying impulse turbine. The combination of airflows from multiple columns was theorised to have the ability to produce a stable and reliable flow of electricity from an 'off the shelf' generator.

Development of the MOWC concept during this contract has then centred on the identification of the ability of the prototype to generate a semi self-regulated flow of energy from which a stable and reliable flow of electricity could be produced. This ability is represented by the regulation of airflow through a self-rectifying turbine, from which a rotational force can be generated and electrical power produced.

The MOWC prototype was initially developed and constructed within the framework of a European Union CRAFT project, (Contract number: JOR3-CT98-7026). The prototype represented the largest wave energy device to be deployed in the United Kingdom since the failure of the Wavegen OSPREY in 1995.

The CRAFT involved the research and development of a broadband sea power energy recovery device by a consortium of companies and a number of Universities from across Europe. The Universities acted as research and technical developers to the company consortium, which was in turn responsible for the exploitation of the technology developed. The results of this project can be read in the project final report, available from the European commission [1].

The aim of this initial project was the construction, deployment and evaluation of a prototype device in the marine environment. This prototype would include an onboard monitoring system that would record the internal water surface motions, air pressures and temperatures. The monitoring system also recorded the physical motions of the device as the incident wave field acted upon it.

This level of data monitoring would allow a full evaluation of the concepts ability to generate a continual and semi self-regulated flow of energy for the production of electrical power.

The project achieved all of its aims and objectives as defined within the CRAFT contract, but a comprehensive evaluation of the sea trials data was inhibited due to technical difficulties. At the culmination of the project, the prototype device had been deployed and was generating a greater level of power than was initially expected. The prototype device was deployed and maintained by the University of Plymouth on behalf of the consortium.

Funding from the DTI was secured shortly after the culmination of the European Union funded project and consents for a prolonged deployment period was agreed with the local authorities.

Summary of work

In order to meet the aims and objectives of the DTI funded project, the continued deployment of the prototype and collection of the subsequent sea trials data was of paramount importance.

Once on location the prototype was unconstrained in its operation and allowed to operate independently.

During the early stages of the project, an incident occurred requiring the eventual retrieval of the prototype from operation. This allowed a new floatation collar and internal monitoring system to be fitted, with the redeployment of a strengthened mooring system.

The catastrophic failure of the semi-tension mooring system towards the end of the project led to the loss of the prototype. However, without the use of this mooring system the project would have been too costly to complete and the power generated by the prototype uncontrollable.

The mathematical analysis of the sea trials data gathered during the operation of the monitoring system was conducted in three main stages:

(i) an initial analysis of the data to give primary indications for conversion efficiency and to assess the physical data for clarity and accuracy;
(ii) an analysis of the local wave climate and wave power density during the sea trials;
(iii) an analysis of the internal power production.

The initial analysis utilised first principle equations to assess the power conversion of the turbine. This process was used to present an initial indication of the results in order to assess the physical data. The results of this analysis provided calibration information for the raw physical data and initial trends.

Analysis of the wave power density per unit width and power generation across the turbine were conducted independently to ensure clarity of the results.

The analysis of the local wave climate utilised the heave displacement of the prototype, in association with the Response Amplitude Operator (RAO) calculated for a simple spar. These results were then multiplied by the capture width of the prototype in order to identify the power available for conversion.

Analysis of the power conversion incorporated the internal water surface elevation, and the internal and external air pressure and temperature. The thermodynamic flow through the turbine maybe considered as being a typical isentropic process. The flow within the device is assumed to be reversible enabling an ideal comparison between the internal process and the end states. As the air passes from the internal volume to the atmosphere its thermodynamic properties change as in a quasi-steady flow process.

Performance of the broadband oscillating water column prototype

The prototype was designed and constructed to limit the level of power it could produce this was achieved in several ways:

(i) the prototype was held in position by a semi-tension mooring system that allowed the prototype to move almost unrestrained in heave;

(ii) the concept of the device presented a inherently stable structure with a large GM minimising the pitch and roll;

(iii) air motion within the prototype was ducted from the oscillating columns via two right angled bends that served to act as restrictors to the motion of airflow out of and into the oscillating columns;

(iv) an air turbine was used to restrict the airflows within the device and act as a power take off dissipating some of the generated power as heat;

The effects of these four limiting methods were successful in maintaining the power generated by the prototype within controllable limits. As the internal motions and air characteristics within the prototype were recorded, post processing will allow further analysis to be conducted to evaluate the full potential of the concept. If these restrictions had not been included then the conversion efficiency of the prototype would have been higher than calculated.

Analysis of the sea trials data was conducted in order to provide evidence to answer the following questions:

(i) What was the conversion efficiency of the prototype during the sea trials period?
(ii) Did the sea trials period represent a typical yearly average of input waves?
(iii) Could the prototype be altered to increase the conversion efficiency?

Results of the generated by the data analysis presented the following answers:

i. The conversion efficiency of the prototype during the sea trials period was calculated at 34.5%. This represents the power converted from incident wave power for a specific capture width, to power available for conversion across the turbine, i.e. power available for conversion within a generator.

ii. The sea trials period contained dominant wave periods between 2.5 and 10.5 seconds. These dominant wavelengths give a fair representation of a typical yearly average with regard to wave type. However, the percentage occurrence for the test site and for a yearly average is not directly comparable. Further work will be conducted using the conversion efficiency of the individual columns and the prototype compared to the dominant wave period, in order to generate an expected seasonal generation for a variety of input wave climates.

iii. The prototype was allowed to heave relatively freely when induced to do so by the input wave field. For dominant wave periods greater than 3 seconds this effect will reduce the level of power generated by the prototype, as it reduces the potential pressure fluctuation across the base of the oscillating columns. By restricting the motion of the columns to heave, a greater pressure fluctuation across the base of the columns is possible with an associated increase in the conversion efficiency.

Conclusions

The generation of these results and the methodology employed in the design and construction of the MOWC prototype ensured that the project was able to meet its aims and objectives.

The data analysis of the sea trials period showed that the concept has the ability to generate high conversion efficiencies. Combination of multiple columns through a single self-rectifying air turbine provides the concept with a method by which the device can withstand storm loading, while continuing to efficiently generate electrical power during low and nominal periods of wave activity.

Comparison of the power generated to that of the power incident upon the prototype shows that the power generated by the device did not rise much above 10kW, even though the input power reached as high as 70kW. The prototype generated a greater level of power during storm periods, but this increased power generation did not present any danger.

This effect is also represented in the comparison of the conversion efficiency of the individual columns and the overall prototype. Results showed that the prototype had greater conversion efficiency when generating power from a wave climate that incorporated an underlying short wave period. This effect is the partial result of allowing the prototype to heave; the prototype has an increased heave motion when experiencing incident wave periods between 2.5 and 3 seconds.

However, this trend is continued over a wide range of dominant wave periods, it is not confined to the short wave period only. Results from efficiency calculations also showed peaks of efficiency within the range of input wave periods. The highest of these occurs at a wave period of approximately 6 seconds. This wave period corresponds closely to the resonant wave period for a 7m column as estimated by mathematical modeling. Other efficiency peaks are shown in this data, but these were not as pronounce.

These results show that the association of the underlying input dominant wave period and the draught of the oscillating column are predictable. The concept represents the potential for a highly efficient device that can not only generate electrical power in periods of nominal wave power, but that can also withstand storm periods without the need for sophisticated control systems to bleed off the excess power generated.

Recommendations

The data has shown the potential of the concept, but further analysis of the sea trials data is required if a full understanding of the internal processes is to be achieved. It is recommended that further analysis of the data first consider removing the heave component from the power generation. This would give the conversion efficiency of a fixed device allowing a simplification of the mooring and cable connection required by a large-scale unit. It would also increase the pressure fluctuation across the base of the oscillating columns and so increase the conversion potential of the concept.

Once the conversion efficiency of a fixed system has been established, the conversion efficiency of the oscillating columns can be addressed individually to identify their conversion efficiencies at different input wave periods. This analysis will allow the conversion efficiency of multiple column draughts to be calculated. These results can then be used to assess the number of columns that would present the optimum number for the efficient conversion of wave energy with regard to deployment locations worldwide.

CONTENTS

LIST OF FIGURES

LIST OF TABLES

LIST OF PLATES

NOMENCLATURE

P = power (W)
ρ = density
g = acceleration due to gravity
a = wave amplitude
z = depth measured negatively downwards
h = water depth
k = wave number, $2\pi/\lambda$
x = horizontal co-ordinate
ω = angular frequency, $2\pi/T$
t = time
Φ = a random phase
l = column draught
f = frequency
T_E = total energy period
m_0 = moment of the spectral density function, $m_0 = \int_0^\infty s(f)df$, total variance of the wave spectrum
W = watts
$\dot{m}$ = mass flow rate
C_p = specific heat capacity, 1.11 J/kgK
T = temperature
C = air velocity
γ = constant
C_d = discharge coefficient
A_0 = orifice area
R = Specific gas constant

1.0 INTRODUCTION

The Department of Trade and Industry (DTI) contracted the University of Plymouth to prolong the deployment of its prototype Multiple Oscillating Water Column (MOWC) wave energy. The prolongation of the sea trials period allowed the generation of physical data from which an evaluation of the concept and an estimation of the overall conversion efficiency achieved during the sea trials period.

This report gives a brief background to the origins of the prototype device and presents the methodology of the MOWC concept.

1.1 Background

The integration of a renewable energy generator into an electrical distribution grid requires the flow of electricity to be maintained within specific limits of voltage and cycles. The ability of a renewable energy system to generate a stable and reliable flow of electricity is therefore of paramount importance to its commercial success.

Development of the MOWC concept during this contract has then centred on the identification of the ability of the prototype to generate a semi self-regulated flow of energy from which a stable and reliable flow of electricity could be produced. This ability is represented by the regulation of airflow through a self-rectifying turbine, from which a rotational force can be generated and electrical power produced.

1.1.1 Development of the MOWC prototype

The MOWC prototype was initially developed and constructed within the framework of a European Union CRAFT project, (Contract number: JOR3-CT98-7026). The prototype represented the largest wave energy device to be deployed in the United Kingdom since the failure of the Wavegen OSPREY in 1995. This project involved the research and development of a broadband sea power energy recovery device by a consortium of companies and a number of Universities from across Europe. The Universities acted as research and technical developers to the company consortium, which was in turn responsible for the exploitation of the technology developed. The results of this project can be read in the project final report, available from the European
commission [1].

The aim of this initial project was the construction, deployment and evaluation of a prototype device in the marine environment. This prototype would include a onboard monitoring system that would record the internal water surface motions, air pressures and temperatures. The monitoring system also recorded the physical motions of the device as the incident wave field acted upon it.

This level of data monitoring would allow a full evaluation of the concepts ability to generate a continual and semi self-regulated flow of energy for the production of electrical power.
The project achieved all of its aims and objectives as defined within the CRAFT contract, but a comprehensive evaluation of the sea trials data was inhibited due to technical difficulties. At the culmination of the project, the prototype device had been deployed and was generating a greater level of power than was initially expected. The prototype device was deployed and maintained by the University of Plymouth on behalf of the consortium.

Funding from the DTI was secured shortly after the culmination of the European Union funded project and consents for a prolonged deployment was agreed with the local authorities.

1.2 Aims and Objectives

1.2.1 Aims

(v) To complete a full analysis of the sea trials data with regard to the incident wave power and power generated across the turbine.

(vi) To evaluate the MOWC concept with regard to the conversion efficiency.

(vii) To recommend future areas of research and development that would increase the conversion efficiency of the concept design.

(viii) To present the physical data into the public domain on a web based site.

1.2.2 Objectives

(iv) The continued deployment of the prototype MOWC prototype for a further period of 12 months.

(v) The evaluation of the MOWC concept in its ability to generate a stable and reliable power for the production of electricity within predefined limits.

(vi) To recommend improvements that could be made to the prototype design in order to increase the conversion efficiency.

2.0 SINGLE OSCILLATING WATER COLUMN

2.1 Introduction

Single chamber oscillating water columns (OWCs) have been the most successful wave energy conversion method to be tested as prototypes. The OWC is a simple and efficient method of converting oscillatory water wave motion into a usable form of energy. The development of this concept has taken two fundamental forms; the fixed caisson (the unit width absorber) and the suspended column (the point absorber).

2.2 Shore mounted fixed caisson oscillating water columns

The caisson OWC consists of a seabed or shore mounted collection chamber designed to convert a waves' surging motion into an oscillatory airflow. This type of prototype includes the LIMPET and Mighty Whale, as well as the concept prototypes such as OSPREY and WASP. These prototypes operate by matching an enclosed mass of water to specific characteristics of wave period and amplitude. When the caisson is subjected to a wave that matches these characteristics the internal mass of water oscillates in harmony with the incident wave.

As the wave periods acting on the caisson become shorter or longer than that desired for optimum wave to wire efficiency, so the characteristics of the oscillatory airflows generated change in both volumetric airflow and pressure. The change in the airflow characteristics results in a loss of conversion efficiency within the turbine and consequently fluctuations in the voltage and frequency of the electrical power generated.

2.3 Single chamber (suspended column) oscillating water columns

The suspended OWC normally consists of a single cylindrical column hung vertically in the water, open at its base. As water waves pass the column, pressure fluctuations in the surrounding water generate a pressure difference across its base, resulting in an internal oscillation.

The pressure fluctuation for a given depth is given by equation 1[2]:

$$p = \rho g a \frac{\cosh(z+h)}{\cosh kh} \sin(kx - \omega t - \Phi) \qquad (1)$$

As with the caisson OWC, there is a specific wave period and amplitude at which the internal mass of water will act in harmony with the external pressure fluctuations. At this wave period and amplitude the water mass within the column will oscillate to its maximum extent, thus generating the maximum volumetric airflow to and from the column to atmosphere. A basic representation of this relationship can be given to be $\omega^2 = g/l$, where l is the column of the draught [3].

2.4 Oscillating water columns; three stages of energy conversion

The OWC can be considered as the primary of three stages for the efficient conversion of water wave motion into electrical power. The physical structure of an OWC simply converts

the motion of a water wave into an oscillation of an air mass in the same manner as a simple piston. As the piston rises within a column it will exhaust air from the top, as the piston is withdrawn, air is sucked back into the column to replenish the partial vacuum created.

The conversion of the potential energy contained within the airflow into a useable form is usually achieved by means of a self-rectifying air turbine, converting the oscillatory motion into a rotational force. The final stage of extraction is achieved by converting this rotational force transmitted through a shaft into electrical power within an electrical generator, figure 2.1.

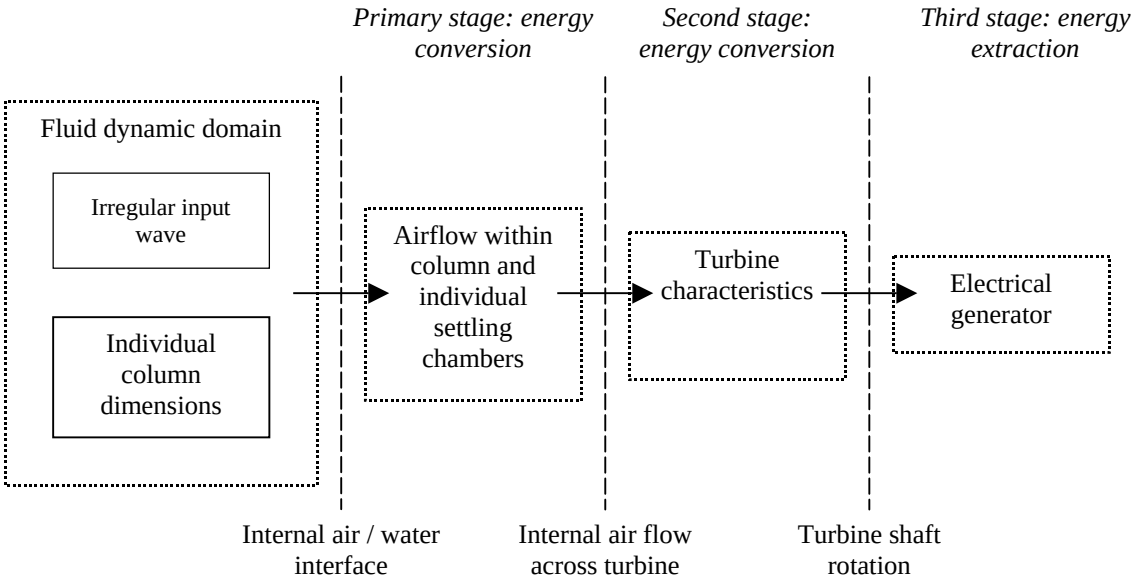

Figure 2.1, a schematic of the three internal domains within an OWC and the process of electrical power generation from water surface motion to electricity generation

The schematic illustrates the need to design any wave energy conversion system with consideration of not only the operational properties of the individual components, but how these components will interact and operate as an entire system.

Air turbines require specific airflow characteristics at which they will operate at their optimum efficiency. As the airflow characteristics across the turbine diminish below or above this operational envelope, the conversion efficiency of the turbine will be affected.

The traditional turbine used in the conversion of an oscillating airflow into a rotational force has been the ‘Wells’ turbine. Development of this turbine introduced a simplification of the oscillating water column system by removing the need to incorporate mechanical flap valves to direct the airflow to the intake side of a mono-directional air turbine. The impulse turbine was also under development at the same time as the ‘Wells’ turbine, but was not successful in becoming widely accepted as a suitable alternative. First presented by Babinsten in 1975, it was not until 1999 that any significant work had been conducted in assessing the potential of the impulse turbine for the conversion of oscillating airflows into a rotational force.

This work presented efficiency and start up characteristic curves for the impulse turbine and a direct comparison with a ‘Wells’ turbine of similar power generation [4]. These curves showed

that the impulse turbine possessed a greater range of efficiency than the 'Wells' and gave better start up characteristics due to the use of external stator vanes.

However, the successful use of any air turbine relies upon the production of an airflow that remains within the operational limits of the turbine. If the airflow characteristics fall below or rise above the operational limit, then a loss of efficiency will result. By using a turbine that has a wide operational envelope the range of these limits can be increased, but the reduction of the operational range incident on the turbine will have a greater increase in the overall conversion efficiency of the system.

Waves acting upon an OWC in a marine environment can be considered as highly non-linear, with regard to period and amplitude. Therefore the airflow characteristics that these input waves create will also be non-linear. As a non-linear wave field passes a wave energy device, the waveform will include an underlying dominant wave period. It is these underlying dominant wave periods to which the device will be matched.

The wave characteristics at which a single OWC will operate at its optimum are experienced sporadically, if the column has been accurately matched to the predominant wave climate. This intermittent occurrence results in the potential for large fluctuations in the airflow characteristics generated within the column. During periods of optimal operation, a high level of power generation is possible, but these high levels may be combined with substantially longer periods of poor power generation.

These erratic fluctuations in electricity generation have made wave energy unattractive to commercial investors and the national transmission and distribution networks. Therefore, there is a need for a constant and secure generation method that uses water wave motion as the instrument from which a stable and continuous airflow can be generated. The concept of the MOWC was envisaged to achieve this objective through the combination of existing techniques and an innovative approach.

As previously discussed, a point absorbing single OWC operates at its optimum efficiency for wave periods and amplitudes close to that at which its internal water mass reacts in harmony with external wave induced pressure fluctuations. This optimum operational harmony is a direct relationship between the draught of the OWC and the incident wave period and amplitude; the greater the draught of the column the longer the wave period to which this harmony will be in effect. It was proposed that a combination of OWCs of different draughts, whose airflows are ducted through a single self rectifying turbine, would generate a combined airflow with a greater stability and smaller range of volumetric flow rate. This combination would therefore present a greater potential for the generation of a stable and reliable supply of electrical power.

2.5 Oscillating water columns; cycle and prototype optimisation

The combination of OWCs presents several indefinable scenarios that are extremely problematic to simulate in both physical tank testing and theoretically.

As an OWC reacts to an external pressure fluctuation it produces an oscillation of the water surface within the column that in turn produces a venting and intake of air from and to the column.

As the air moves from column to atmosphere and back, it is acted upon by the turbine as it passes through the blades. This action restricts the passing of the air creating a backpressure on the up stroke as air is driven out and a partial vacuum on the downward stroke as the air endeavours to return. These effects impede the motion of the water surface as it moves up and down within the column.

The effect of this water surface - air cushion - turbine interaction can accurately be modelled if the following are known:

(i) the pressure fluctuations across the base of the column;
(ii) the motion of the internal water mass due to the pressure fluctuations at its base;
(iii) the fluid and thermodynamic effects of the oscillating water surface on the internal air cushion;
(iv) the motion of the air through the turbine and the internal transfer of energy;
(v) the external air pressure;

From these parameters the motion of the water surface can be simulated to a high degree of accuracy using first principle linear theory within the time domain. However, indefinable non-linear properties are introduced when two or more OWCs are combined through a single air turbine.

As discussed, oscillation of the internal water mass is the product of the external pressure fluctuations across the base of the column. The composition of this oscillation is dissimilar for incident waves with periods shorter or longer than that of resonance.

An oscillating column can be considered to have a two stroke cycle, figure 2.2. As the pressure increases across its base the water within the column is forced upwards, as this pressure is reduced a hydrostatic restoring force causes the water mass to recede.

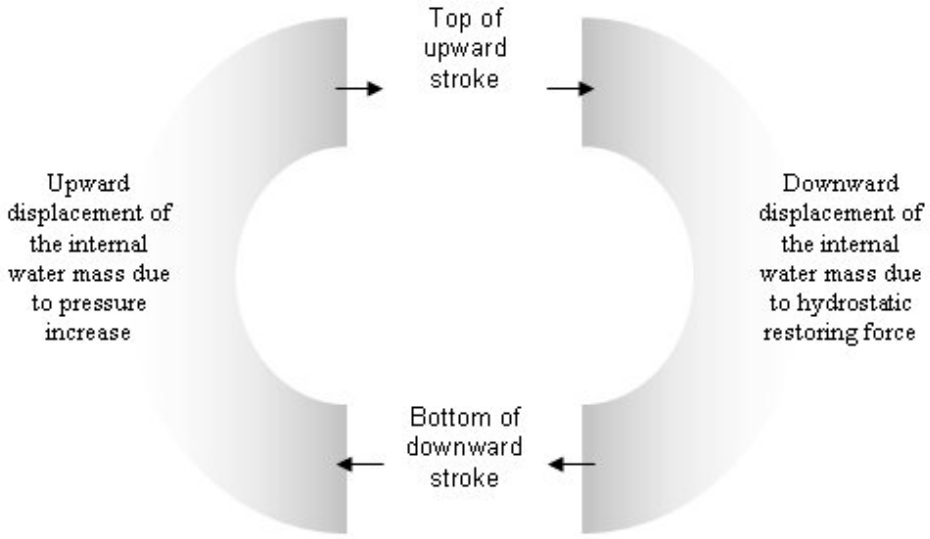

Figure 2.2, cycle of internal water mass

The optimisation of the internal cycle is achieved by matching the potential motion of the internal water mass to the cyclic motion of an external wave field. An enclosed mass of water

will have an optimum cycle at which it will act in harmony with the external wave, generating a resonance within the column.

Wave periods that are shorter than that of the optimum, result in a net loss of energy transfer as the interactions between the pressure fluctuations and the oscillation's enclosed mass of water act in partial opposition. Longer period waves generate pressure fluctuations over a greater time period, exerting their influence on the internal water surface in a more protracted manner.

For Long period input waves the internal water surface follows the external input, figure 2.3. When incident of short period waves, the internal water surface oscillates, but to less of an extent when compared to the external water surface, figure 2.4.

When a column is affected by a wave that corresponds to its resonance wave period, the internal water surface oscillates in harmony with the pressure fluctuation. This effect can create an oscillation of greater amplitude that the external input wave, with the internal oscillation follow a ¼ wavelength, or a phase angle of 90^0, behind that of the input wave, figure 2.5.

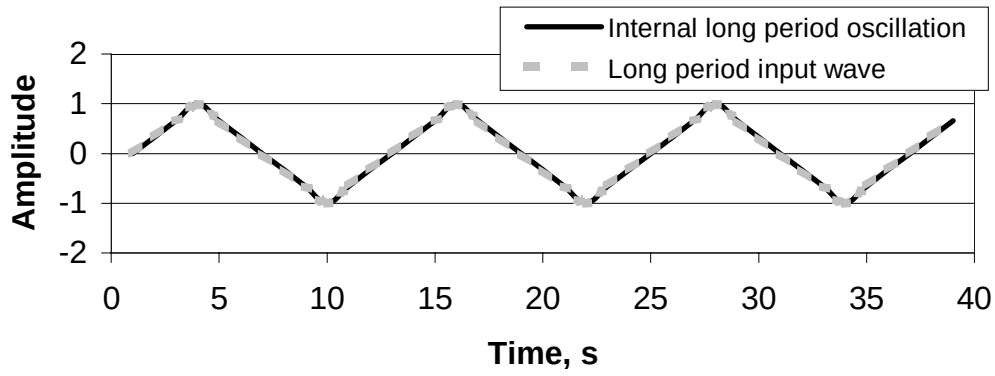

Figure 2.3, a monochromatic long input wave period and the resultant internal waver surface oscillation

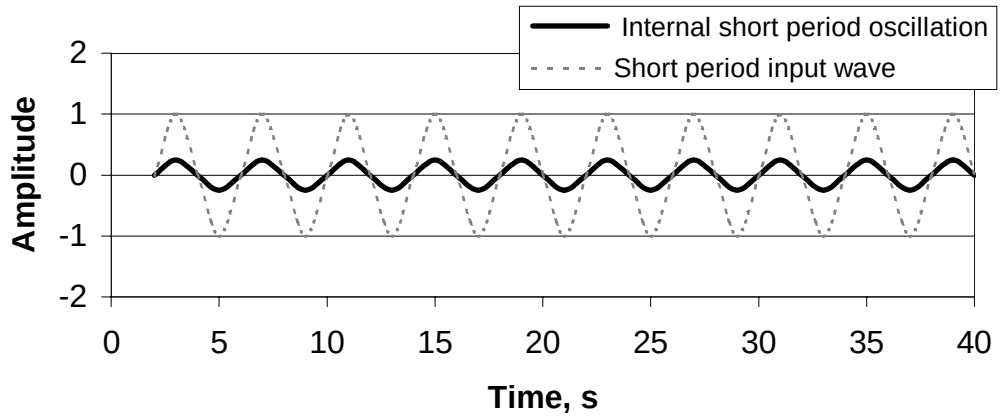

Figure 2.4, a monochromatic short input wave period and the resultant internal waver surface oscillation

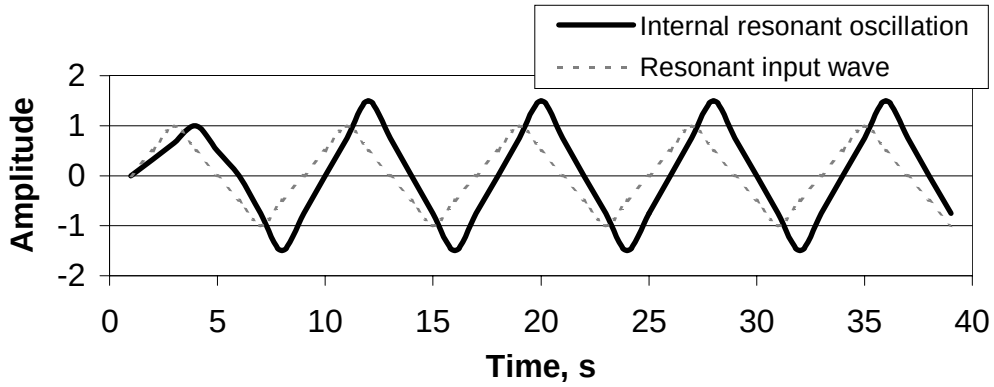

Figure 2.5, a monochromatic resonant input wave period and the resultant internal waver surface oscillation

The depth to which a wave will induce a pressure fluctuation in the water column is a function of its wave number, which in turn is a function of the wavelength. The longer the wavelength the greater the depth to which a pressure fluctuation will be experienced. This characteristic is the method used to match columns of differing draughts to specific wave periods.

Oscillations of a water surface within an undamped column assume that there are no restrictions on the passage of air. When an air turbine is included it restricts the airflow, thus imposing a dampening on the internal motion. This dampening reduces the harmonic frequency of the internal water surface resulting in an associated increase in the resonant wave period.

When assuming the inclusion of an air turbine the increase of the wave period is dependant upon the level of dampening placed on the passage of air. The restriction of the airflow is a function of the turbines physical characteristics and its speed of rotation.

The physical restriction is generated as the air is ducted into the turbine through the stator blades and passes across the rotor blades. The dampening imposed by the rotor blades is reduced as the rotational speed of the turbine increases. Within a single OWC the dampening placed on the internal water mass oscillates as the airflows are continually reversed.

The dampening created by a single airflow can be modelled using linear theory as the characteristics of the turbine can be identified. As the air is forced into the turbine the pressure within the column rises. This backpressure continues to increase as the column rises and forms a classic feed forward – feed back model, figure 2.6.

When multiple columns are combined this classic system becomes increasingly complicated with regards to the modelling of the stochastic interactions between the individual columns through the single air turbine, figure 2.7.

The use of linear theory introduces a large number of simplifying limits that in turn results in the generation of data, which does not represent the physical system. This limitation has presented several problems during the development of the MOWC prototype, but will be overcome by the generation of physical data derived from large-scale sea trials.

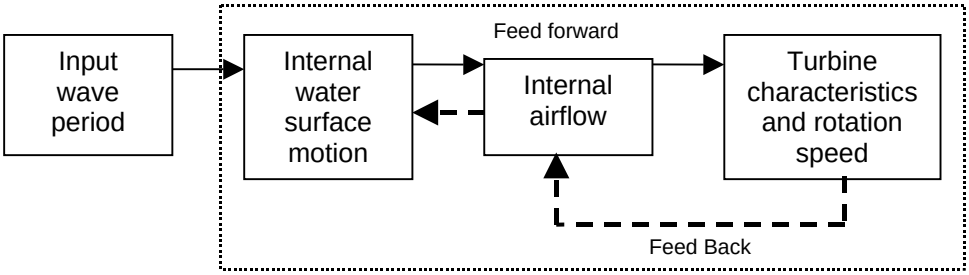

Figure 2.6, a diagram of the feed forward – feed back relationship within a single column OWC

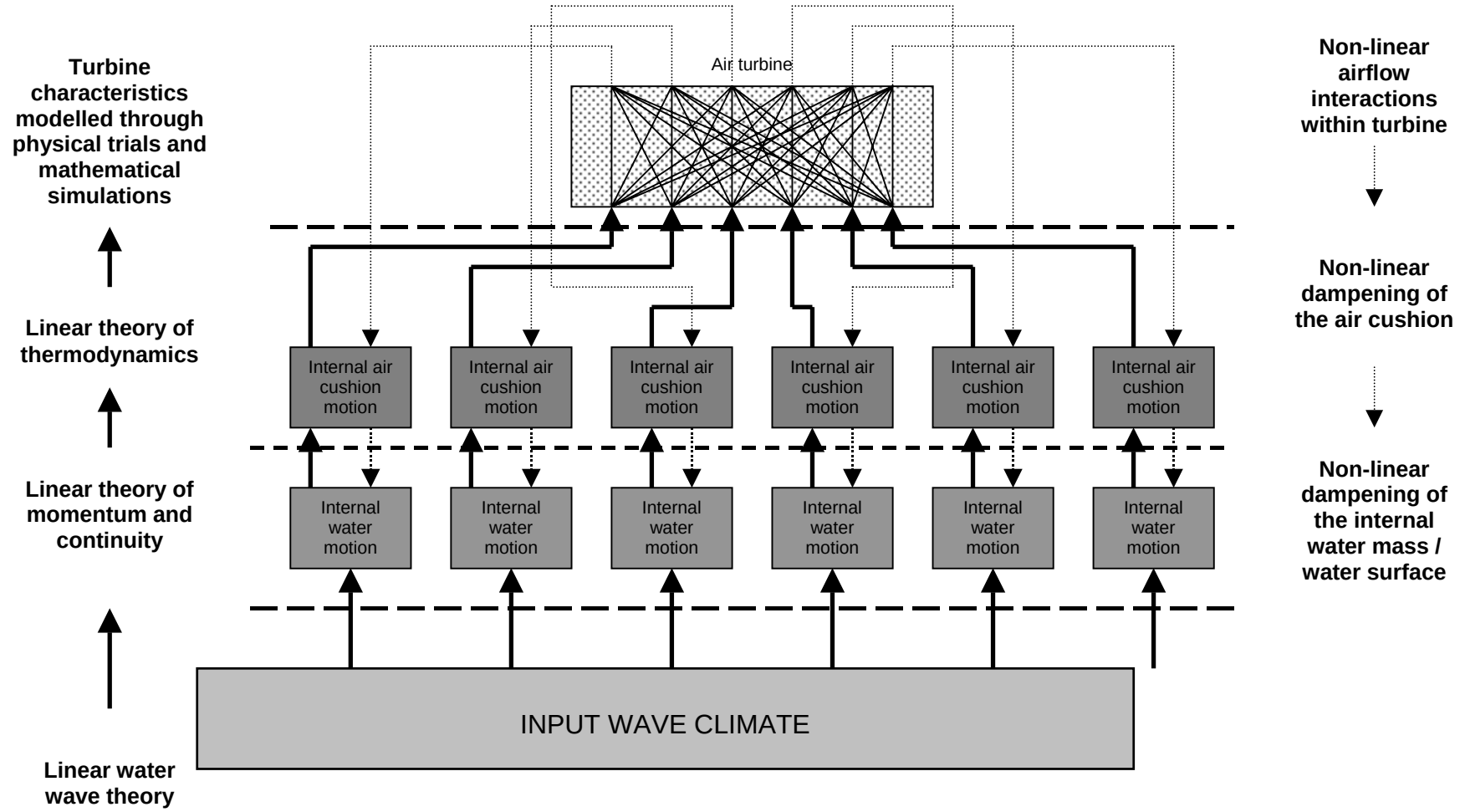

Figure 2.7, feed forward – feed back system representing a 6 column multiple oscillating water column wave energy device

3.0 SIMULATION OF A SINGLE FIXED OSCILLATING WATER COLUMN

3.1 Introduction

Single and multiple column fixed and floating OWCs have been simulated using both mathematical models and physical tank tests. Results have been compared to assess the ability of both the methods to accurately depict the motions of a full size OWC.

Tank testing was conducted using a single fixed undamped column, with a diameter of 50mm, subjected to a range of monochromatic wave periods with a constant wave height, plate 1.

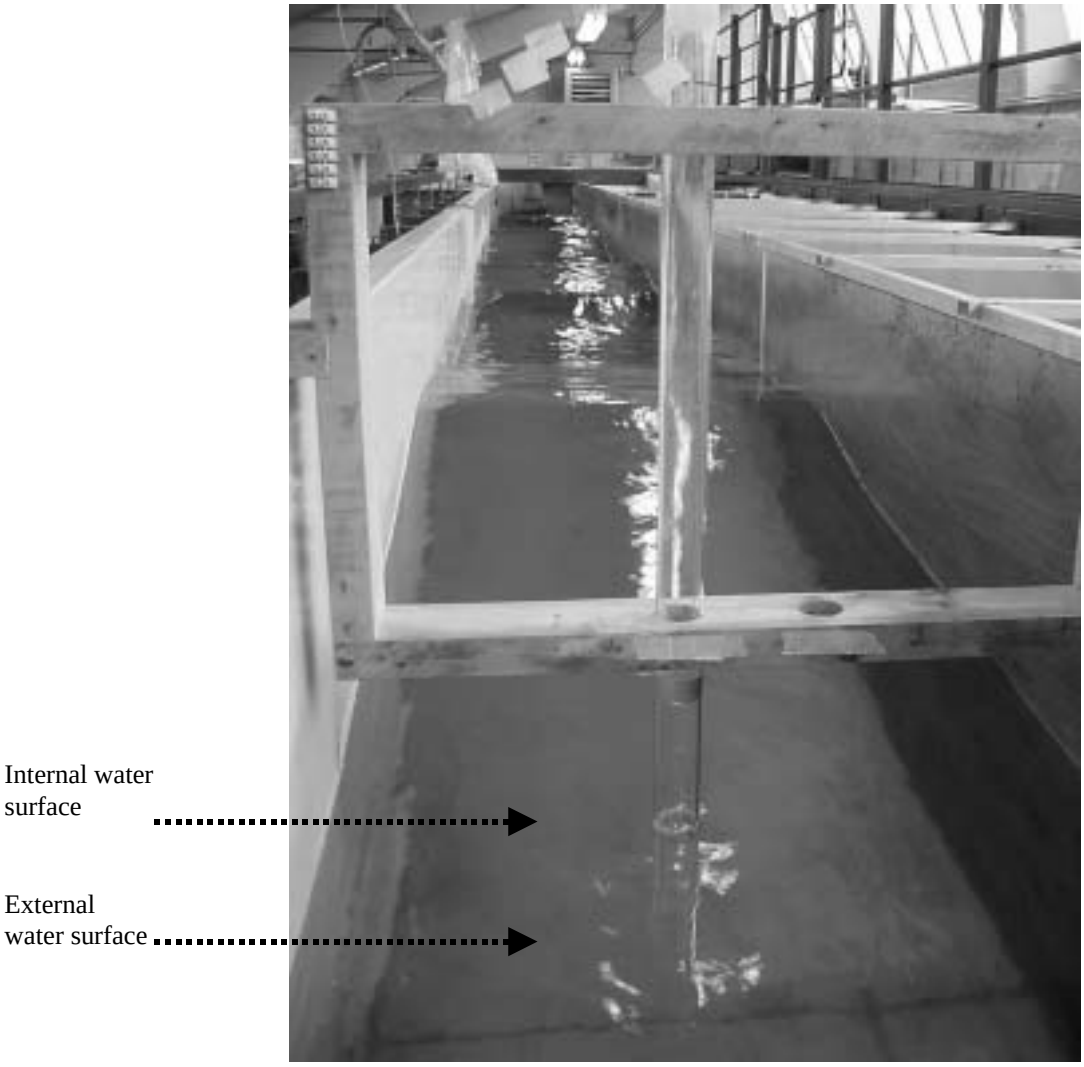

Plate 1, tank testing of a single fixed column conducted in a flume tank at the University of Plymouth

3.2 Test parameters and results

Multiple runs were conducted over a range of column draughts to establish the instantaneous internal and external motions of the water surfaces, figure 3.1. These results showed that a single fixed undamped column exhibited a potential to generate internal oscillations with amplitudes several times greater than that of the input wave, but over relatively short bandwidths.

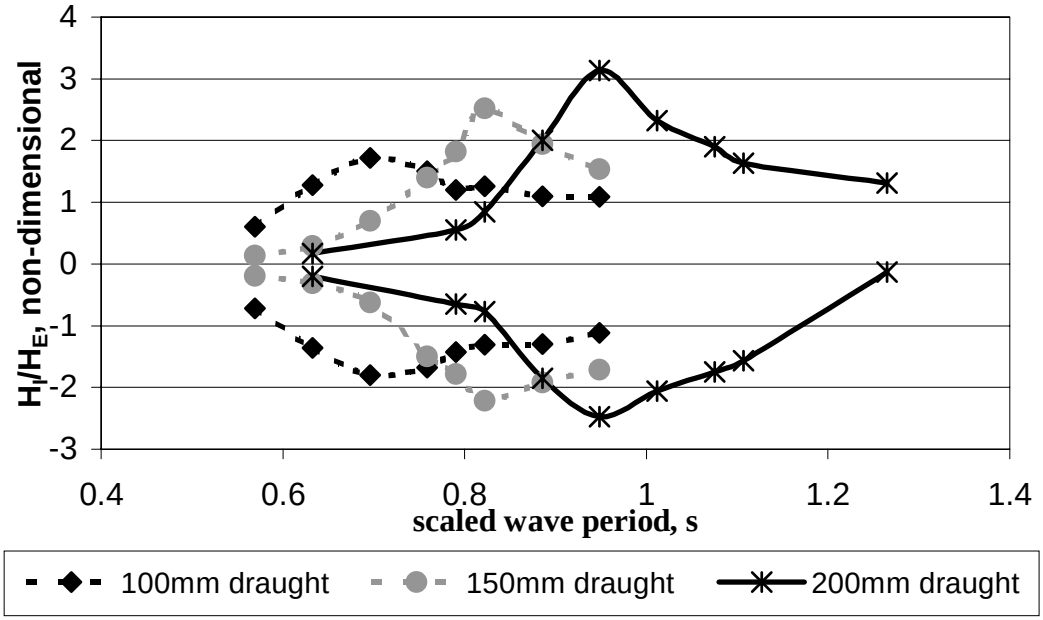

Figure 3.1, the peak and trough relationships between the internal and external water surfaces elevations for 3 separate columns draughts, (H_I – Internal wave height, H_E – External wave height, scaling is consistent with froude)

3.3 Discussion

It can be shown both physically and through equation 1 that shorter wavelengths induce pressure fluctuations to a lesser depth than that of a longer wavelength .

$$P = \rho g a \frac{\cosh(z+h)}{\cosh kh} \sin(kx - \omega t - \Phi) \qquad (1)$$

As discussed it has been shown that the shorter than resonance wave periods generate internal oscillations with amplitudes lower than that of the input wave amplitude. When wave periods longer than that of resonance are experienced, the pressure fluctuations across the base of the column take place at a rate that allows the internal water surface to react in total sympathy. Resonance is experienced when the pressure fluctuations generated by the incident wave cause a harmonic amplification of the water mass contained within the column.

If the results shown in figure 3.1 are scaled up to represent a 10m column then the corresponding resonant wave period would be between 6.7 and 7.4 seconds. Mathematical simulations gave a resonant wave period of 6.5 seconds for a fixed undamped column, figure 3.2.

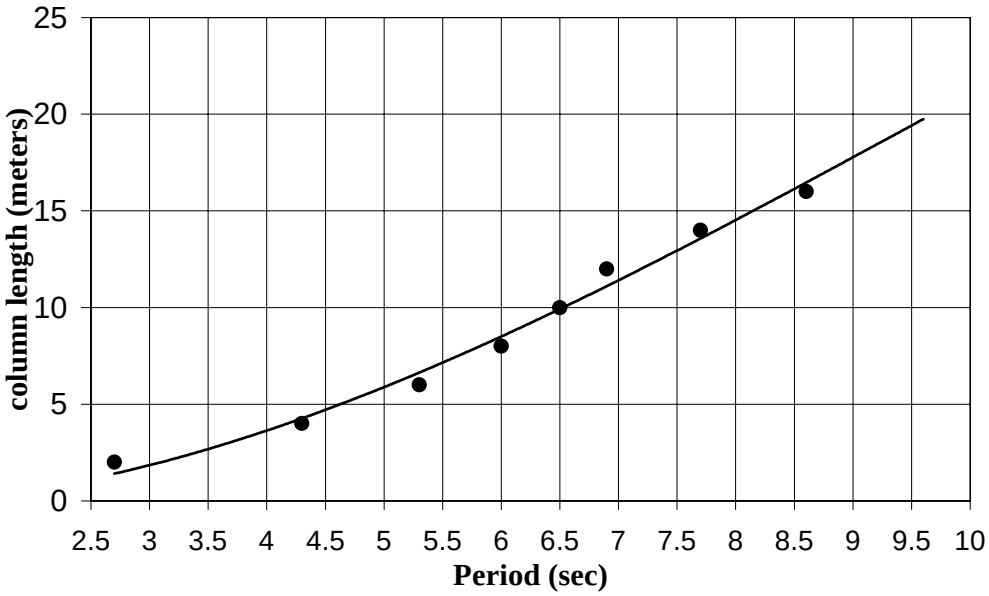

Figure 3.2, the mathematically modelled relationship of resonance between a column draught and the monochromatic input wave

The data used in this comparison was generated within the scope of this DTI contract; comparisons were also conducted with the simulation results of the mathematical model and data generated in the prior European Union funded CRAFT project. This physical study was conducted by the Hydraulics and Maritime Research Centre, University College Cork. The content of this report is confidential and cannot be discussed here in full, however it can be noted that these comparisons generated equivocal results to those obtained and presented within this report.

4.0 MULTIPLE OSCILLATING WATER COLUMN

4.1 Introduction

The ability of a single OWC to collect and convert water wave and surge motion into an oscillatory airflow has been well documented. The MOWC concept incorporates the conversion potential of individual OWCs within a single turbine in order to increase the bandwidth over which it continues to create airflows that can be efficiently converted to electrical power.

The combination of individual OWCs to vent individually into a single self rectifying turbine was theorised to promote the ability of the configuration to generate a stable level of electrical power. This increased ability to convert pressure fluctuations into electrical power over an increased bandwidth, promotes the MOWC concept over other wave energy systems. A single OWC may produce more power for a specific incident wave, but a MOWC device will have a greater efficiency over a wider bandwidth.

A possible limitation of this concept, and the area of most contention, is the interactions of the airflows generated by individual columns within the turbine. Initial studies have been concentrated on the simulation of a single cylindrical fixed OWC subjected to monochromatic waves in both undamped and damped configurations.

These simulations showed that a fixed undamped OWC experienced a resonance of the internal water mass specific to a particular wave period. The results of this work were also used to compare the internal water surface motion with that of the external; as the water within the column oscillates it lags behind that of the external.

This change in phase between the internal and external water surface, before, during and after resonance is one of the internal effects through which the MOWC device will generate a reduced range of airflows over a greater bandwidth of incident wave periods (wavelength) and amplitudes (wave height).

4.2 Internal mass flow rate for single and multiple columns.

As the water surfaces within the prototype oscillate they lag behind the motions of the external water surface. By selecting the correct column draughts for a specific site and wave climate the individual airflows can be combined to produce airflows with greater regularity and stability to which a self rectifying air turbine can be designed.

The analysis of the data from the 24th January 2002 between 21:03 and 21:23 shows the mass flow rates of the 3 oscillating columns contains large fluctuation, figure 4.1-4.3. When these airflows combine within the turbine they create airflow with a greater regularity and less high frequency variation, figure 4.4.

This effect reduces the range of the operational envelope over which the turbine must operate and increases the turbines' efficiency in producing a stable flow of electricity. Note that the mass

flow is not shown as negative as the passage of air in both directions contributes to a continual rotation of the turbine in the same direction.

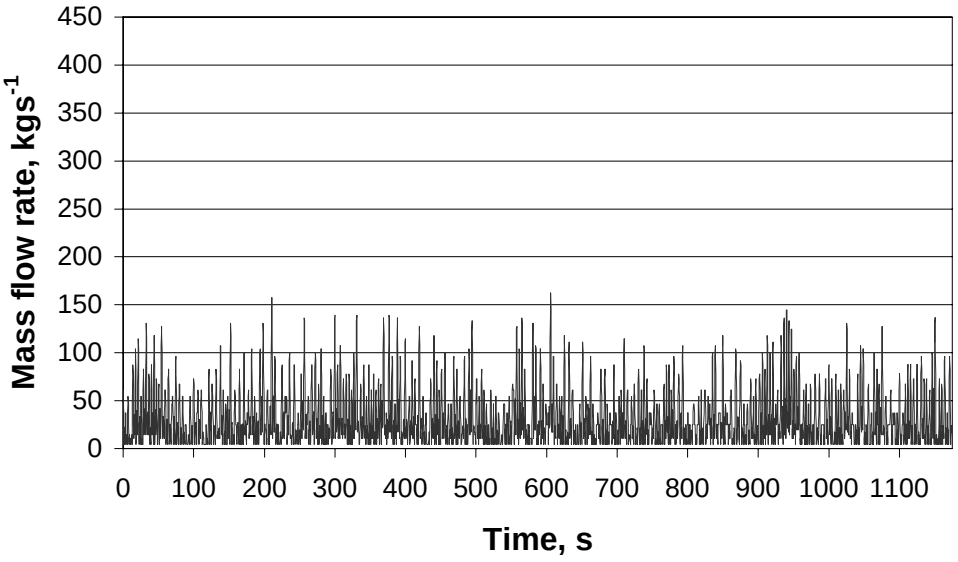

Figure 4.1, mass flow rate generated by column 1 between 2103-2123 on the 24th January

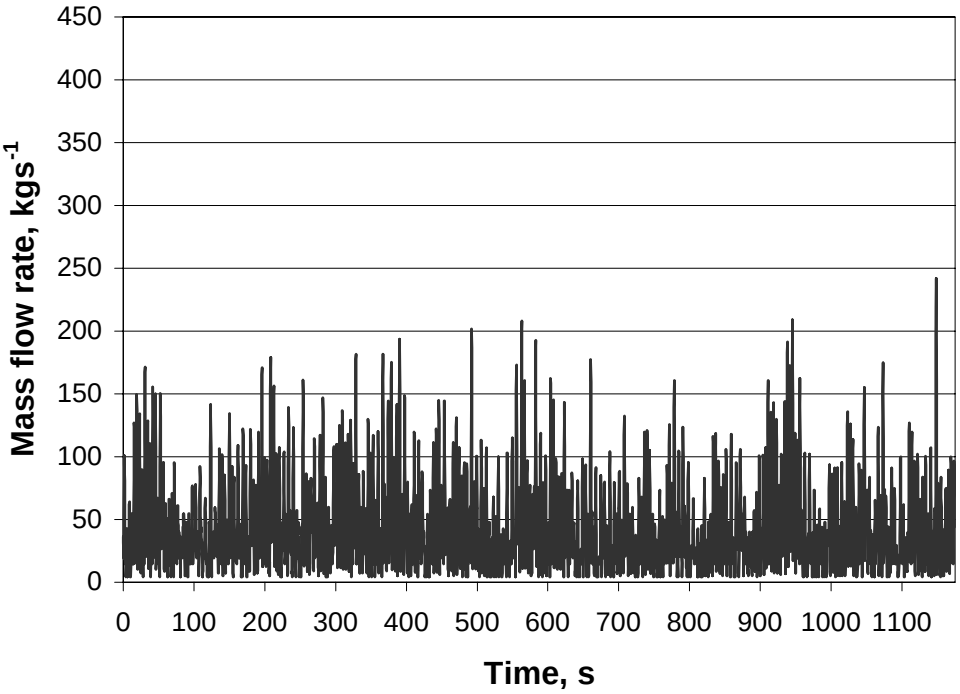

Figure 4.2, mass flow rate generated by column 2 between 2103-2123 on the 24th January 2002

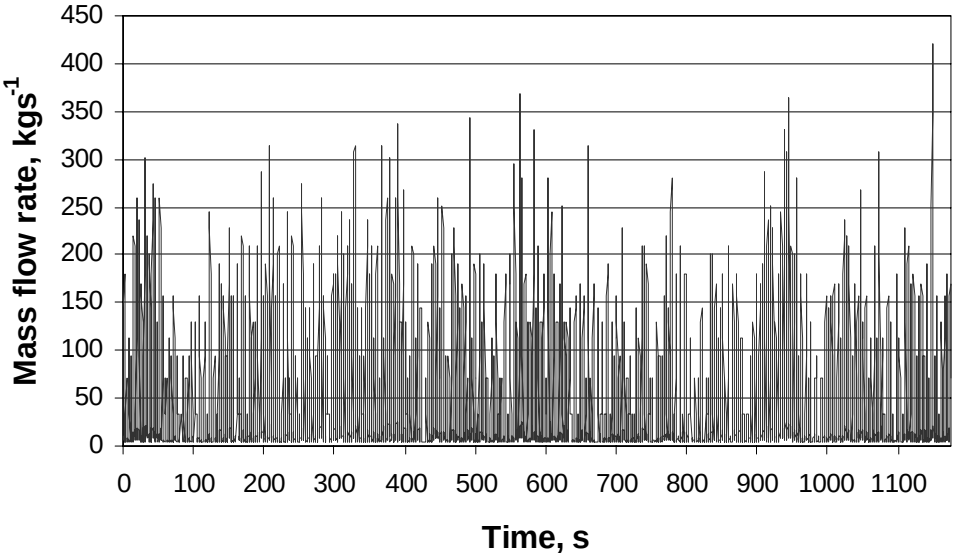

Figure 4.3, mass flow rate generated by column 3 between 2103-2123 on the 24th January 2002

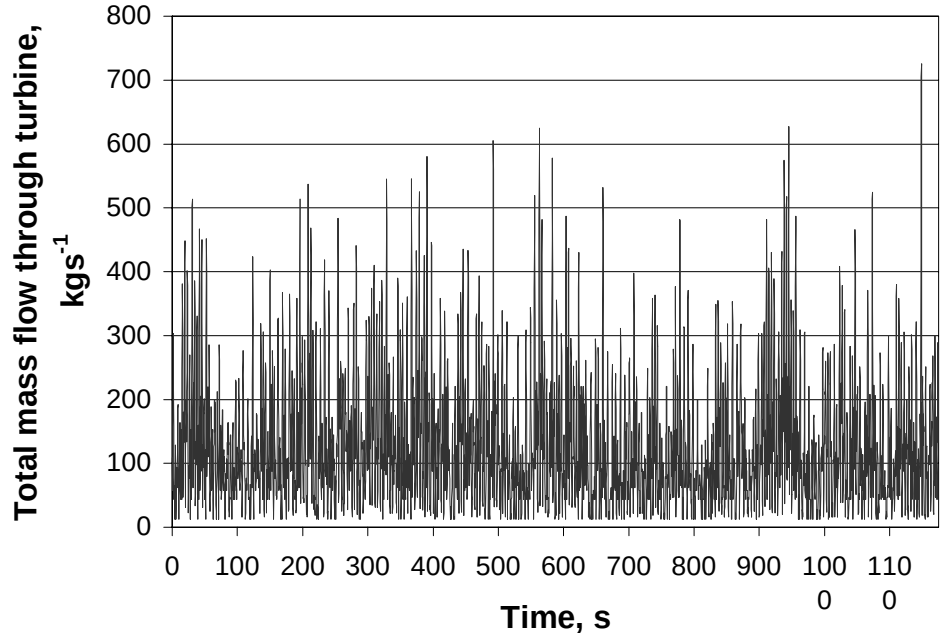

Figure 4.4, total mass flow rate passing through turbine between 2103-2123 on the 24th January 2002

The combination of the airflows within the turbine generates a greater mass flow rate with an increased stability over a wider bandwidth of incident waves than would be generated by a single column of equivalent internal air volume. This achievement increases the capacity of the system to supply electricity over a wider bandwidth. Figure 4.4 shows the combination of only 3 columns, as more columns are introduced the resulting combined mass flow rates continue to become more stable.

5.0 EXPERIMENTAL PROTOTYPE AND PHYSICAL SEA TRIALS

5.1 Introduction

The experimental prototype was initially funded by the European Commission Joule Thermie Non-Nuclear Energy Programme. The project ran from the 1st January 1999 until the 28th February 2001 and was conducted as a European Union CRAFT project. This combined technical research from academic institutions and the commercial exploitation of industrial partners.

The project combined the abilities of 4 industrial partners and 3 university institutions from across Europe.

(i) Cornish Steel Ltd, UK
(ii) Embley Energy Ltd, UK
(iii) Hippo Marine Products Ltd, UK
(iv) IBK, Germany
(v) Chalmers University of Technology, Sweden
(vi) University College Cork, Eire
(vii) University of Plymouth, UK

The research and development was co-ordinated within the University of Plymouth with industrial co-ordination and obligatory exploitation activities being co-ordinated by Embley Energy Ltd.

The project was the first stage technical feasibility study of a broadband seapower energy recovery device. The aim of the project was the evaluation and validation of a concept through the analysis of physical data generated by a prototype wave energy device during sea trials conducted off the South west coast of the United Kingdom.

The areas of development within this project included:

(i) analysis of single and multiple OWC motion;
(ii) identification and design of a suitable conversion turbine;
(iii) regional and site-specific wave statistics and characterisation;
(iv) tank testing of scale models;
(v) hydrodynamic motion and mooring system;
(vi) electrical power generation and dissipation;
(vii) materials selection and construction methods;
(viii) monitoring and recording of prototype performance and data telemetry;
(ix) commercial exploitation of the projects outcome;

The research and development conducted within the project identified a design that would meet the projects requirement of generating electrical power from a broad bandwidth of input waves. The project considered several variations of a multiple oscillating water column system. However, after additional analysis it was decided that the configuration most suitable incorporated multiple columns of different draughts and a single self-rectifying air turbine. This

design also represented the best design for simplicity and mechanical strength to withstand the rigours of the marine environment.

The additional analysis considered further concepts including;

(i) flap valves to direct internal airflows;
(ii) datum columns suspended to the still water level and placed at the rear of the turbine with the aim of increasing the pressure difference across the turbine;
(iii) dampening plates hung beneath the prototype to restrict heave motion;
(iv) an encapsulating bell chamber incorporating water seals around the prototype to assist in the conversion of heave motion into airflow;
(v) multiple turbines located on each column with either a single or multiple generators;
(vi) floats located within the columns from which their motion can be used to generate electrical power;
(vii) inclusion of venturi chambers to increase the flow of water within the columns;

All of these additional options were considered and discounted on the recommendation of the academic institutes and Embley Energy Ltd.

5.2 Experimental prototype

The experimental prototype consisted of four columns suspended vertically below the water surface. This configuration included three oscillating columns of different draughts and a single datum column for modelling and analysis calibration. The three oscillating columns were ducted into individual settling chambers and separately into a single self-rectifying impulse turbine connected to a drive shaft and generator representing a resistive load, figure 5.1.

This configuration allowed the interactions between multiple stochastic components of the MOWC to be monitored for later analysis. As the prototype was developed within a first stage technical feasibility study several unknowns were identified during development. These included:

(i) the effect of combining multiple airflows;
(ii) the oscillatory dampening effect placed on the internal water surface by the turbine;
(iii) the interaction of the multiple columns through the turbine interaction;
(iv) the effect of air compression within the columns on the hydrodynamic characteristics of the prototype;

It was also identified that the motion of the prototype at sea could have a profound effect on the efficiency of the design as the prototype heaves, pitches and rolls. As the monitoring of this motion was possible, it was decided to include a mooring system designed to have a limited effect upon the heave of the prototype while restricting the motion in the other five degrees of freedom. The motion of the device could then be used as a secondary measure of the incident wave climate.

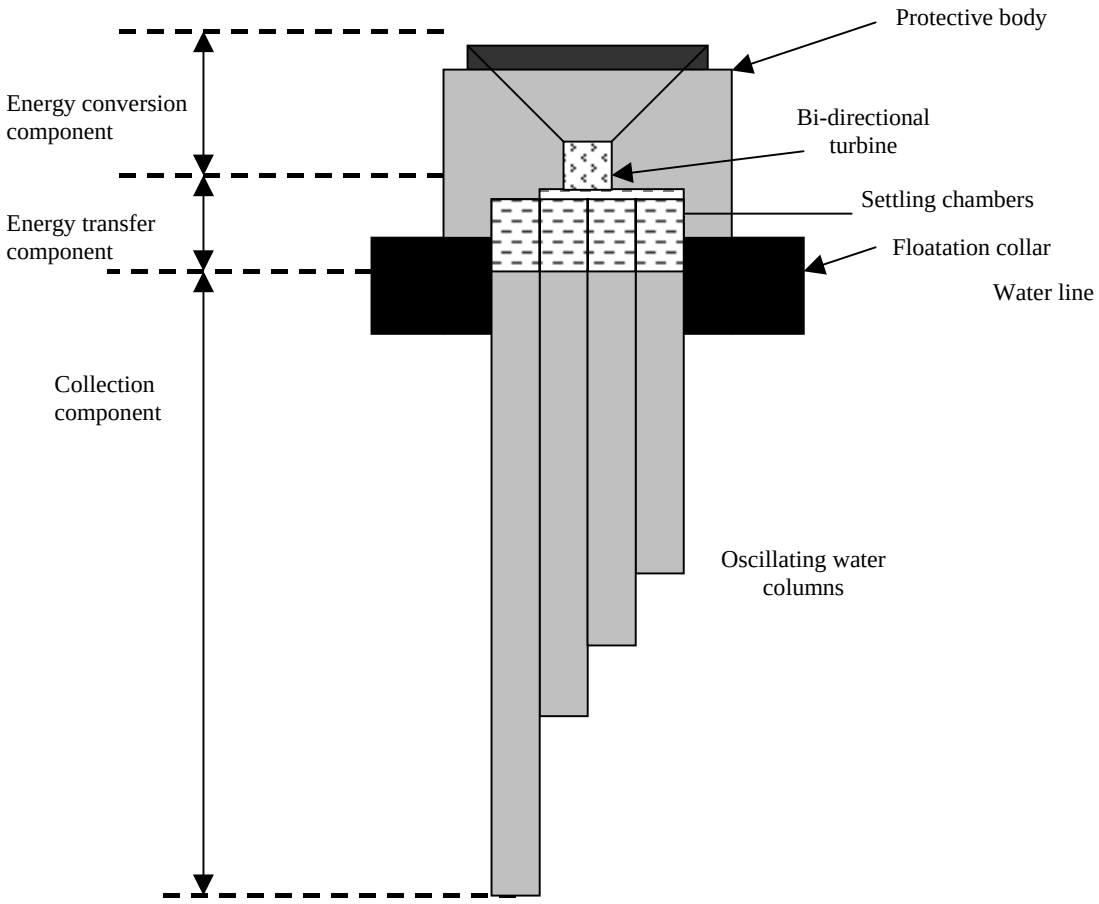

Figure 5.1, Schematic of the floating MOWC prototype, showing primary equipment and main components

5.3 Mooring system and deployment location

This mooring system was developed in association with Chalmers University of Technology, Sweden, who also conducted a full analysis of the prototype hydrodynamic motions.

The mooring system consisted of three identical arms, figure 5.2, each comprising of a sea bed holding weight and a tension riser wire secured to a surface buoy that was in turn secured to the prototype on the water line.

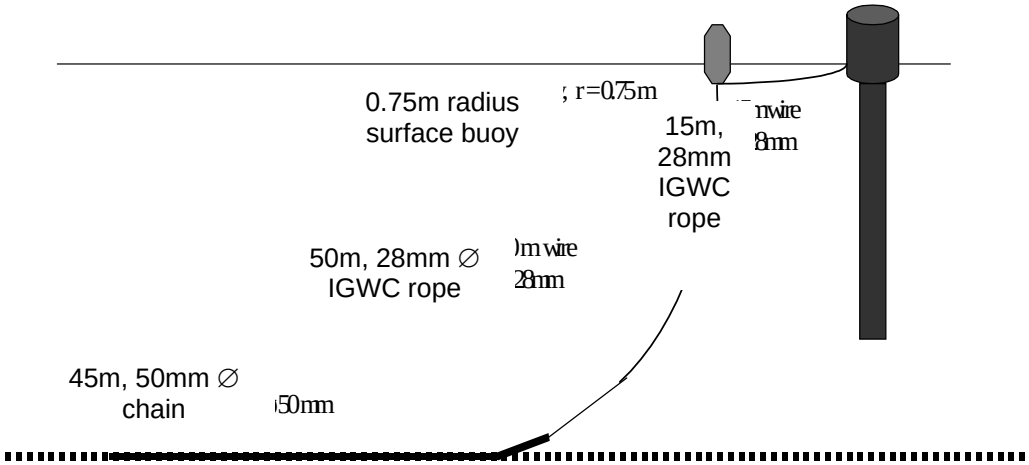

Figure 5.2, a schematic of a single mooring arm

Due to the predominance of the local weather from the southwest it was decided to increase the holding capacity of the south westerly mooring by increasing the length and subsequent weight of the ground chain by an additional 50m.

The deployment location of the prototype was restricted to the confines of the Port of Plymouth Dockyard Limit. This restriction was due to navigational risks, insurance and the achievement of consents from the Crown Estate and local authorities. The prototype was deployed in 18m of water (chart datum) in a position agreed with the Queens Harbour Master, figure 5.3.

The central position was agreed as (OSGB36):

LAT:	50^0 18’ 56.4000” N	(DD MM SS.SSSS)
LONG:	004^0 8’ 36.0000” W	(DD MM SS.SSSS)

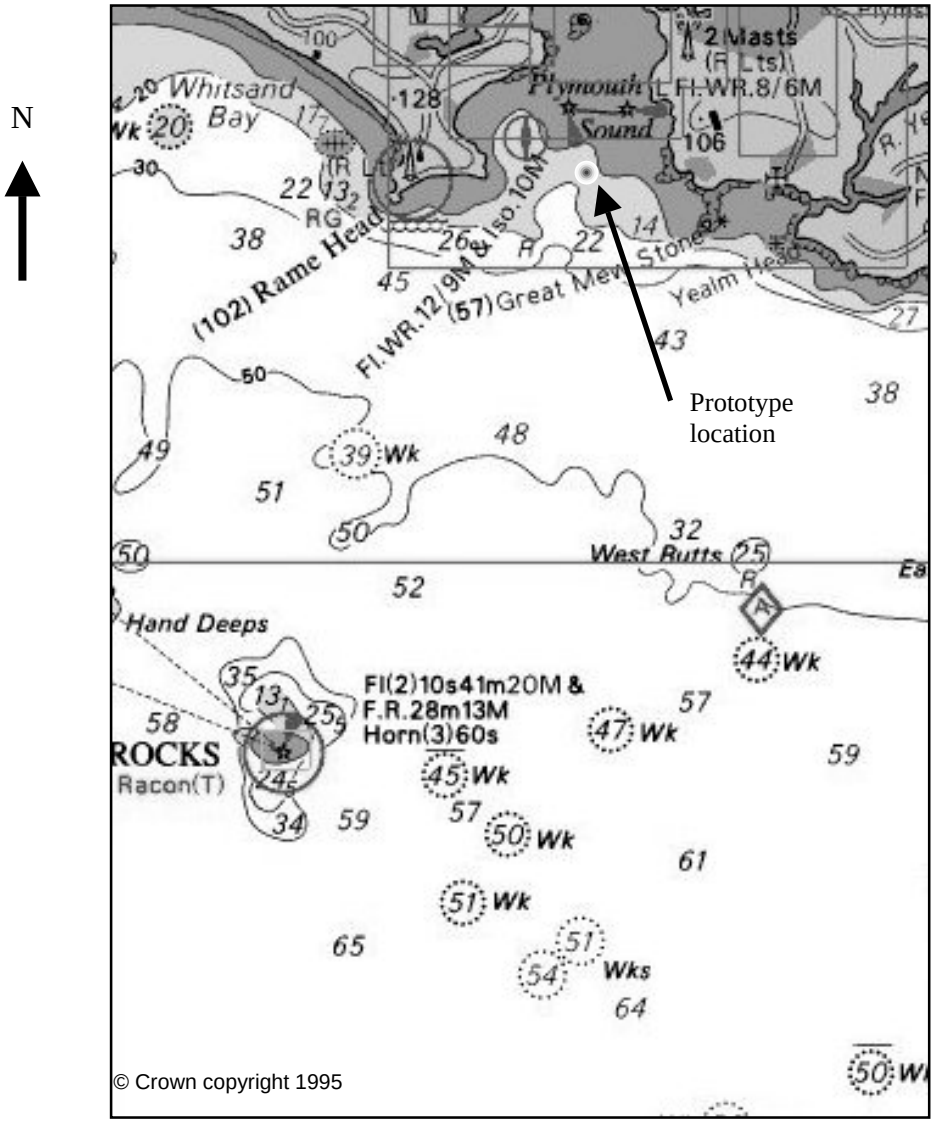

Figure 5.3, the prototype location within the confines of the Port of Plymouth Dock Yard Limit

5.4 Sea trials

The prototype was first deployed on the 28th February 2001 within the remit of the EU CRAFT project. Cornish Steel Ltd at Hayle in Cornwall constructed the prototype as a modular unit. The modular design was required due to height and width restrictions during its transportation from the construction facility to the assembly and deployment site in Plymouth.

Construction of the prototype was approved by Embley Energy Ltd. on behalf of the industrial collaborators, with much of the prototype being supplied as “in kind contribution” to the project. This situation resulted in a high level of interaction between university staff and the industrial

collaborators to ensure that the prototype was constructed to the required engineering specifications.

After the initial deployment of the prototype, the onboard monitoring system was only partially installed due to component malfunctions. Prior to its complete installation the prototype suffered an unknown incident, likely to have been a collision, that left the prototype secured to only two mooring wires. One of the mooring wires was ripped from the prototype at its connection to the surface buoy and on closer inspection it was observed that a section of floatation collar had been damaged.

As previously discussed the mooring system is designed to operate in tension. Once a mooring arm had been lost the system became slack allowing the prototype greater scope to move in the horizontal.

During a maintenance inspection it was observed that the surface mooring wires were coming into contact with the floatation collar. This collar was constructed of glass re-enforced plastic with a polystyrene core. Its resistance to the wear of the 28mm steel cable was therefore limited.

As the prototype ranged within the moorings it placed an alternating load on each. This motion eventually intertwined the two moorings bringing them together. Consequently one of the surface mooring wires was wrapped around the floatation collar, causing it to bite into the collar with every surge. This situation lead to the floatation collar becoming badly damaged and the decision was made to recover the prototype prior to its possible loss.

While ashore the prototype device was broken up into two separate units, the upper body and the column structure. Work conducted while the prototype was ashore included:

(i) re-antifouling of the columns;
(ii) re-painting of the exterior and interior of the upper structure;
(iii) replacement of company and university logos;
(iv) replacement of safety wires;
(v) reconstruction and calibration of monitoring system.;
(vi) removal and rebalancing of Impulse turbine;
(vii) replacement of generator and power dissipation circuit;
(viii) replacement of floatation collar with protective tyre skirt;
(ix) recovery and reconstruction of mooring system with new wires and surface buoys;
(x) strengthening of datum column piping system.

The prototype was re-launched in co-operation with the Queens Harbour Master in Mid October 2001. The prototype was moored in Barn Pool, a deep water mooring in the entrance to the River Tamar in order that the remaining internal components could be fitted. The onboard monitoring system was replaced during this period with a prolonged test to ensure it was fully functional and calibrated to still water conditions.

The prototype was deemed fully operational in the middle of December 2001 after a 4 week period of continuous monitoring. The moorings were deployed soon after this and the wait for a forecasted calm weather window ensued. Final deployment was achieved on the 16th January, the

first data set generated at the test site at 1800 on the same day. The sub sea wave pressure array was to be deployed in the week following the deployment of the prototype; however this was postponed due to the onset of a prolonged period of rough weather. The rough weather also prevented any access on board the prototype to replace the internal batteries or exchange the data collection flash cards.

This rough period of weather intensified on the morning of the 1st February with conditions becoming extremely hazardous. During this period the mooring system experienced a catastrophic sequential failure allowing the prototype to drift towards the shore. After the failure of the mooring system the prototype remained fully operational while it drifted within the confines of the main port area. Due to the severe weather conditions the Port was closed to all traffic except those under their direct military control. This prevented any recovery operation being mounted and is a decision that has not been made by the Port Authorities in many years.

The prototype ran aground at approximately 12:00; due to the rough conditions Staff from the University were unable to approach the prototype until several days after the grounding. It was not until 10 days after the grounding that the internal monitoring systems, data cards and turbine assembly could be removed.

The only recommendation this report can conclude from the failure of the mooring system is a lesson hard learnt from the offshore industry. When floating structures are allowed to move horizontally, surge, sway and yaw, they can generate substantial levels of momentum; this motion generates large forces and cyclic loading. Many of the installations now built and moored offshore use tension mooring systems to limit the forces a structure can generate as it is acted upon by the incident wave climate.

The aim of the project was the evaluation of the MOWC prototype; the use of the three arm mooring system was to limit the influence of the mooring pattern on the device motion and to reduce the power generation. The mooring pattern achieved this objective, but its failure halted the sea trials of the prototype, however, any future device would include a means by which the device would be constrained to heave. This requirement dictates the use of a tension mooring system, now becoming widely used in the offshore industry, to restrict this heave motion and increase the conversion efficiency of the design.

6.0 DATA COLLECTION AND CALIBTATION

6.1 Introduction

To achieve the evaluation of the internal interactions between the individual OWCs within the MOWC prototype, the following parameters were recorded:

(i) individual internal water surface levels;
(ii) internal air pressures and temperatures;
(iii) atmospheric air pressure;
(iv) turbine rotation speed;
(v) generator voltage output;
(vi) individual battery voltages;

(vii) prototype physical motion (x,y,z);
(viii) exterior wave field;
(ix) internal battery voltage.

These parameters were recorded using a monitoring system designed and constructed at the University of Plymouth, plates 2-6. The monitoring system was designed to give as much insight into the internal workings of the prototype as possible and to ensure that there was sufficient redundancy in the data collected.

Plate 2, the on board monitoring system in its external and waterproof internal casing
Left: 2 12v batteries, top left: small box housing accelerometers. Bottom right: Campbell data logger and flash cards
Top right: control boards with external sensor connections

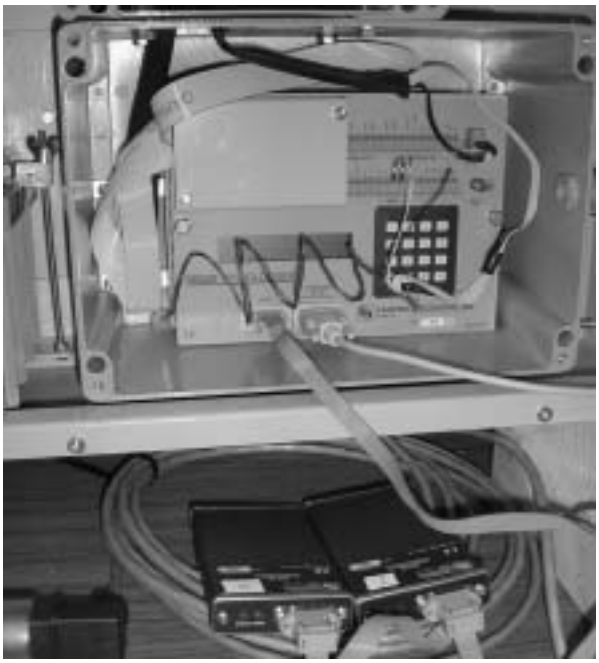

Plate 3, Campbell scientific data logger and 16MB flash cards

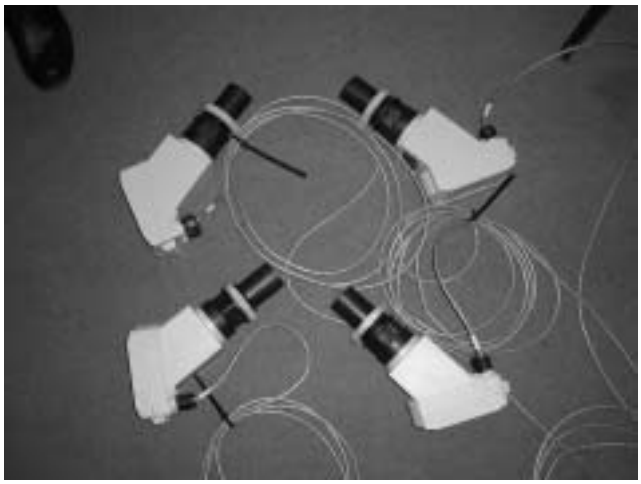

Plate 4, Vega sonic sensors used to measure the internal water level

Plate 5, internal pressure and temperature sensors mounted within a protective housing

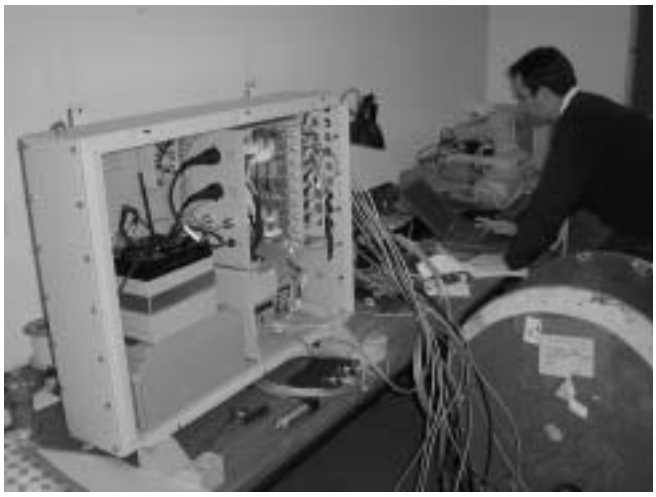

Plate 6, The monitoring and telemetry system undergoing its final test prior to installation

The parameters recorded by the monitoring system, the sensor used and the quality of the data recorded and the level of accuracy that can be expected from each senor are shown in table 6.1. All of the sensors chosen had accuracies far greater than the inherent inaccuracies present when working in a real environment.

Many of the sensors used have a proven record of operating in a marine environment. The sensors that failed to operate after the prototype was fully deployed were initially chosen for their robust nature and operational qualities.

Parameter	Sensor	Record	Comments	Accuracy
Column 1 pressure	Druck, PTX 1830	Full	Good quality data	+- 0.06%
Column 2 Pressure	Druck, PTX 1830	Full	Good quality data	
Column 3 Pressure	Druck, PTX 1830	Full	Good quality data	
Column 4 Pressure	Druck, PTX 1830	Full	Good quality data	
Column 1 level	VEGASON 51K	Full, some noise	Good quality data	+- 0.01%
Column 2 level	VEGASON 51K	Partial	Data record show high levels of noise interference.	
Column 3 level	VEGASON 51K	Full, some noise	Good quality data	
Column 4 level	VEGASON 51K	Partial	Data record shows high levels of noise interference towards the end of the test period.	
Column 1 temperature	---	Full	Temperature sensors prove too slow in responding to the rapid temperature fluctuations experienced within the individual columns. However they do correspond to the general trend between internal and external temperature.	0.1 ^{0}C
Column 2 temperature	---			
Column 3 temperature	---			
Column 4 temperature	---			
Atmospheric pressure	Druck, pressure	Full	Good quality data	+- 0.06%
Shaft RPM	Magnetic encoder	None	Sensor failed to operate	--
Generator output voltage	---	None	Sensor failed to operate	--
Prototype motion Ax	KISTLER 8303A1	Full	Good quality data, but problematic to analyse entirely due to a lack of rate of change sensors.	0.1% / V
Prototype motion Ay	KISTLER 8303A1	Full		
Prototype motion Az	KISTLER 8303A1	Full		
System Voltage 12V	Direct voltage	Full	Showed expected voltage drops during recording period.	--
System Voltage 24V	Direct voltage	Full		
Sub sea pressure A1	Druck, PTX 1830	None	Sub sea pressure array not deployed due to adverse weather conditions and loss of prototype.	+- 0.06%
Sub sea pressure A2	Druck, PTX 1830	None		

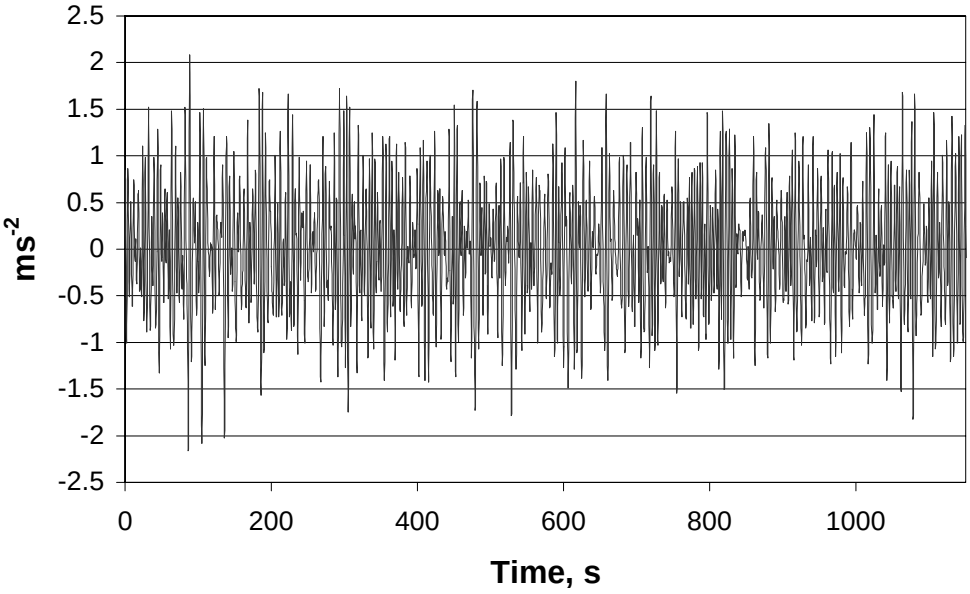

Sub sea pressure A3	Druck, PTX 1830	None		

Table 6.1, parameter recorded, sensor type and quality of data recorded.

6.2 Collection period

Data was recorded by the monitoring system for 20 minutes every 3 hours between 1800 on the 16th January and 0300 on the 1st February 2002. This data is available via the following web address: http//www.tech.plym.ac.uk/sme

6.3 Data calibration.

All of the data generated by the monitoring system was recorded as a voltage reading and then calibrated using an appropriate equation.

6.3.1 Accelerometers

Ax: Vstatic = 2510mV S = 779mV/g
Ay: Vstatic = 2490mV S = 783mV/g
Az: Vstatic = 2770mV S = 592mV/g

Data calibrated relative to gravity $1 = 9.81 ms^{-2} = (U – Vstatic) / S$

The accelerometers record the motions of the prototype with reference to gravity. i.e. a value of 1 is equal to 9.81 ms^{-2}. Equations 2 - 5 were used to convert this recorded data into vertical acceleration, velocity and displacement:

$A_{Z(RAW)} - cons\tan t = A_Z$	relative to gravity	(2)
$A_Z \times G(9.81) = A_z ms^{-2}$	converts to acceleration	(3)
$\partial A_Z \times \partial t = A_{ZV} ms^{-1}$	converts to velocity	(4)
$\partial A_{ZV} \times \partial t = A_{ZD} m$	converts to displacement	(5)

This method of conversion from acceleration with reference to gravity to the actual prototype displacement is shown in figures 6.1 – 6.7.

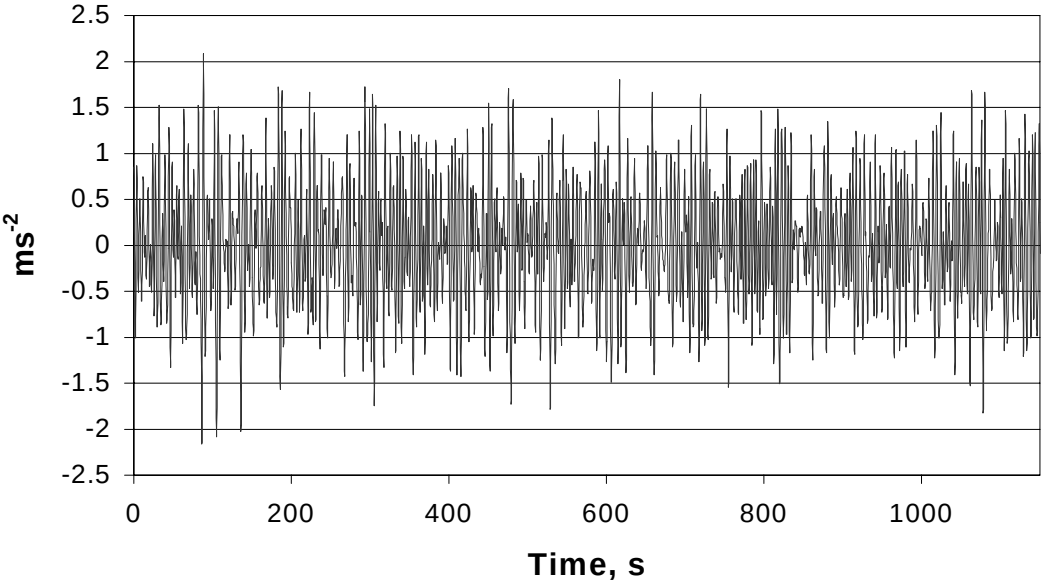

Figure 6.1, prototype acceleration during the sample period: 0003 – 0023: 29th January 2002

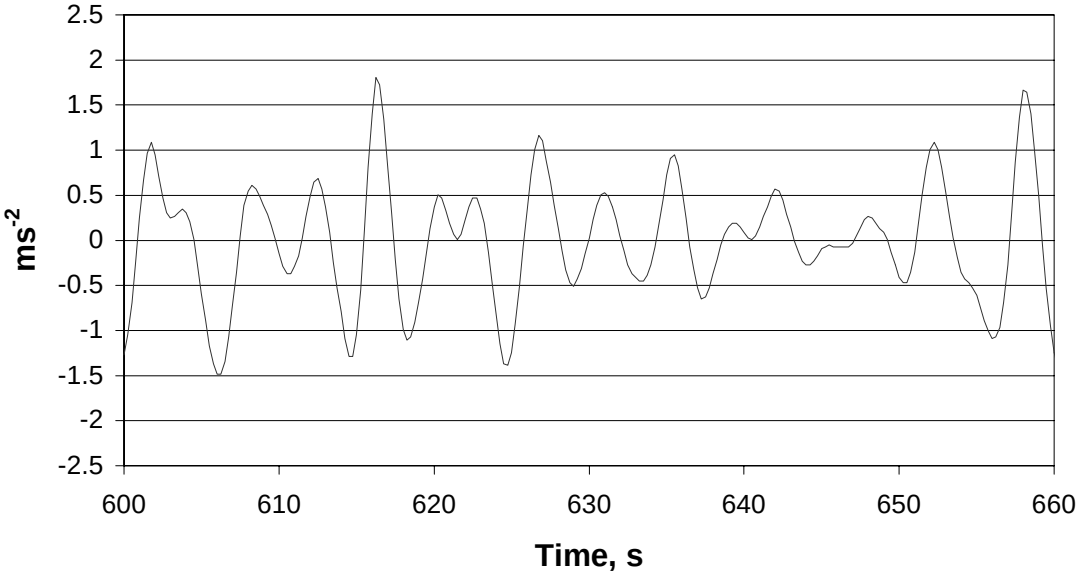

Figure 6.2, prototype acceleration during the sample period: 0013 – 0014: 29th January 2002

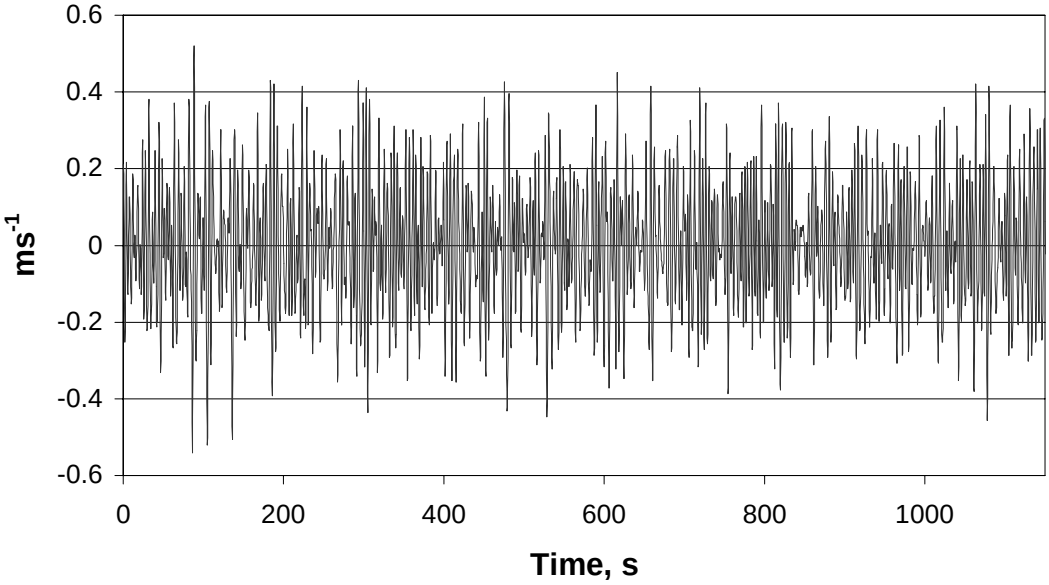

Figure 6.3, prototype velocity during the sample period: 0003 – 0023: 29th January 2002

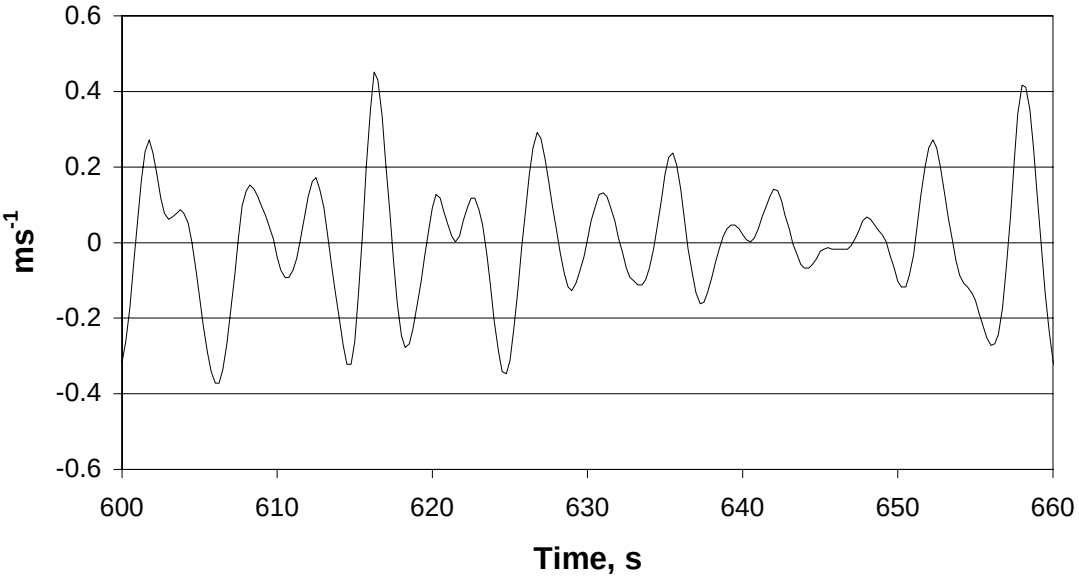

Figure 6.4, prototype velocity during the sample period: 0013 – 0014: 29th January 2002

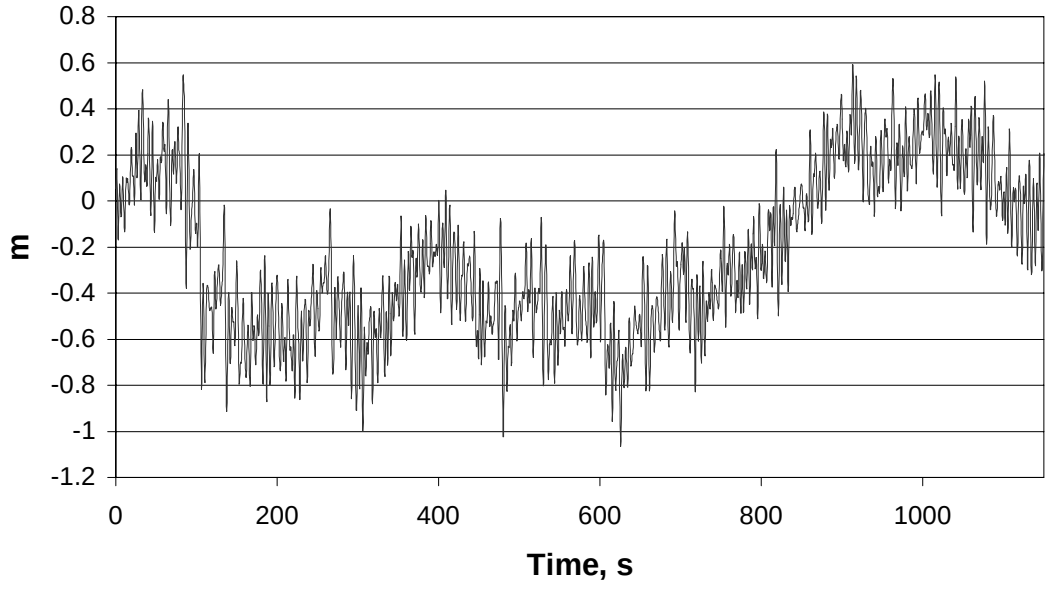

Figure 6.5, prototype displacement during the sample period: 0003 – 0023: 29th January 2002

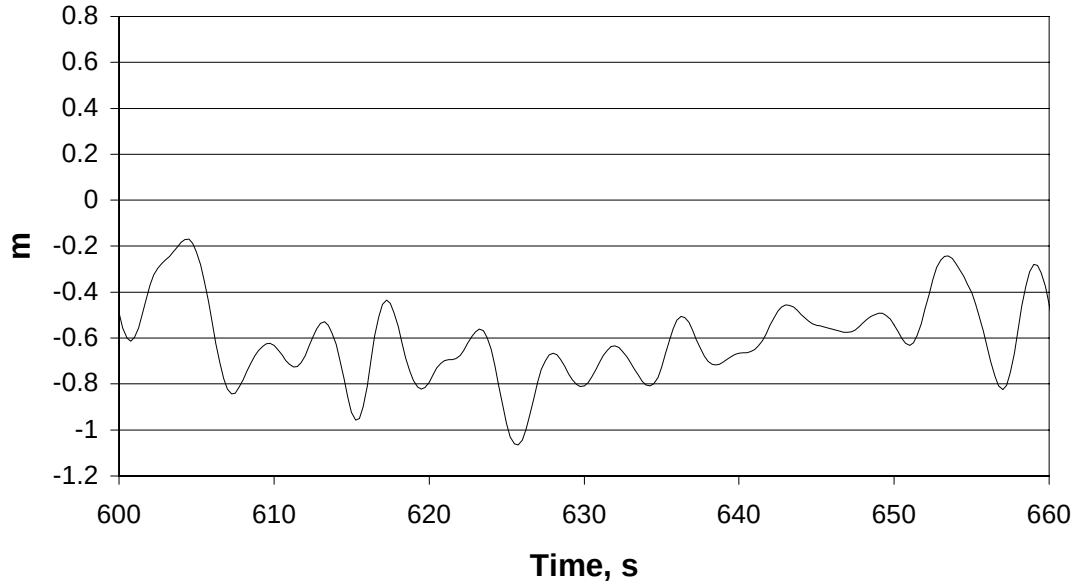

Figure 6.6, prototype displacement during the sample period: 0013 – 0014: 29th January 2002

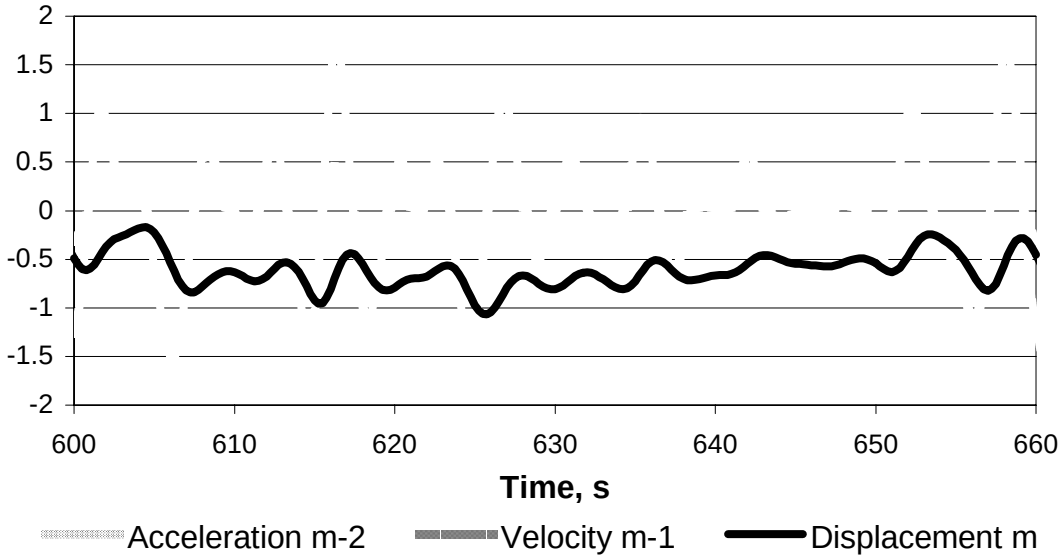

Figure 6.7, prototype acceleration, velocity and displacement during the sample period: 0013 – 0014: 29th January 2002

Figure 6.7 shows the acceleration and velocity having identical phase, while the prototypes displacement lags approximately 90^0 behind. The shift of the displacement away from the zero

datum is caused by inaccuracies in the recording of the acceleration and changes in the physical water surface level due to climatic variations.

6.3.2 Internal water surface level

$$L = (6242 - U) / 1534 \text{ (m from sensing head)} \quad (7)$$

The initial information given by the calibration equation supplies the internal water surface elevation with reference to distance from the sensor, figure 6.8. By subtracting the distance of the sensor from the value given the internal water surface elevation is produced with reference to the still water level, figure 6.9.

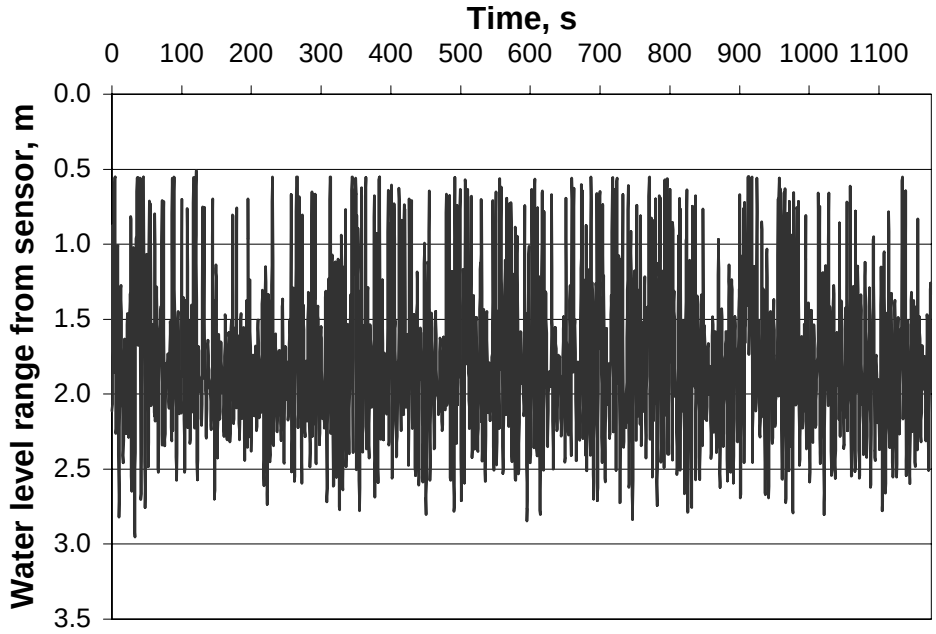

Figure 6.8, internal water surface elevations with reference to the sensor mounting

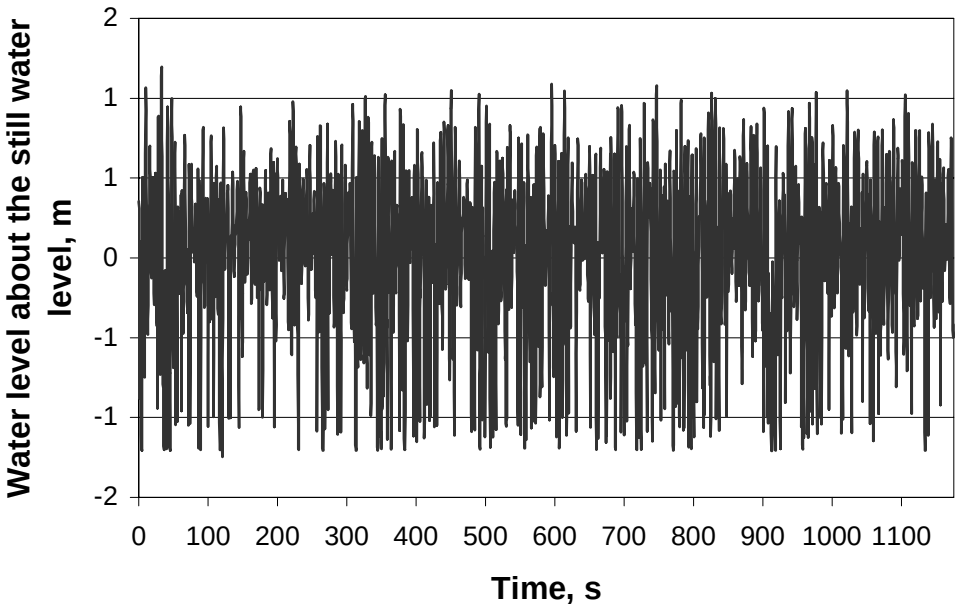

Figure 6.9, internal water surface elevations with reference to the still water level

6.3.3 Air temperature

$$T = (U-3000)/40 \ (C^0, mV) \quad (8)$$

6.3.4 Air pressure

$$P = 0.5 \ (U/1000 - 1) \ (bar, mV) \quad (9)$$

6.4 Data Interpretation

The data recorded by the onboard system was first calibrated to convert the voltage readings into physical internal motions, air pressures and temperatures. The analysis work to be conducted using the data was then divided into four separate areas:

(i) the hydrodynamic motion of the prototype in six degrees of freedom, surge, sway, yaw, roll, heave, and pitch;
(ii) the thermodynamic process within the individual columns and their possible interactions through the turbine;
(iii) the local directional wave climate incident to the test site;

6.4.1 Hydrodynamic motion of the prototype in six degrees of freedom

Analysis of the accelerometers gave the vertical and horizontal motions in three axis. However these results also include the motions of roll, pitch, and sway within the motions recorded in the three axis x,y,z.

As the prototype is acted upon by a wave it will not only experience horizontal and vertical motion, but also a roll and/or a pitching motion. These motions are recorded by the sensors within the horizontal motion and could introduce an error into the data recorded for heave. The extent of this error can be quantified by conducting calculations for the prototypes' hydrodynamic motion. This was conducted for a simple spar system, the unit of m/m is equal to response amplitude / wave amplitude, head seas = 225^0T.

6.4.1.1 Roll motion

Maximum roll motion: 11.2 degrees per meter wave amplitude for beam seas.

6.4.1.2 Pitching motion

Maximum pitching motion: 11.2 degrees per meter wave amplitude at seas +- 45^0 from head seas.

6.4.1.3 Yaw motion

Maximum yaw motion: 9 degrees / meter wave amplitude at $\pm$ 135 degrees from head seas, this direction would be due north or due east.

The prototype was well protected by land from these directions with the maximum off set angle being $\pm$ 90. At these wave directions from head seas the maximum yaw angle would be 2 degrees / meter wave amplitude.

6.4.1.4 Surge motion

The units mm^{-1} represent the non-dimensional units of response amplitude / wave amplitude.

Maximum surge motion: Between 0 and +-45^0.

(i) 0.4 mm^{-1} for wave periods less than 5 seconds.
(ii) 0.8 mm^{-1} for wave periods between 5 and 10 seconds
(iii) 1.2 mm^{-1} for wave periods greater than 10 seconds.

6.4.1.5 Sway motion

Maximum Sway motion: at seas +-90^0.

(i) 0.4 mm^{-1} for wave periods less than 5 seconds.
(ii) 0.8 mm^{-1} for wave periods between 5 and 10 seconds
(iii) 1.2 mm^{-1} for wave periods greater than 10 seconds.

6.4.1.6 Heave motion

Maximum heave: for all sea directions (the spar is circular)

(i) 0 mm^{-1} for wave periods less than 2.5 seconds.
(ii) 0.4 mm^{-1} for wave periods between 2.5 and 4 seconds.
(iii) 0.8 mm^{-1} for wave periods greater than 4 seconds.

The hydrodynamic motion of the prototype can be considered as relatively insignificant when the incident wave period begins to exceed 3.5 seconds.

At wave periods above this level the prototype experiences an almost 1:1 relationship in heave. The prototype also experiences minimal motions in surge, sway and yaw, as the weather affecting the prototype comes predominantly from a south westerly direction. The prototype was deployed with an extended mooring in this direction to inhibit hydrodynamic motion in all degrees except heave.

The direction of the prevailing weather will also inhibit rolling motion, with some pitching being evident as the prototype rides the oncoming seas. However, this component will be low as the prototype was designed to be inherently stable with a high metacentric height and large distance between this point and the centre of gravity making the prototype inherently stiff, Appendix A

6.4.2 Internal air characteristics

The analysis of the internal air motion uses the data from the internal water surface level, internal and external air pressure and the internal and external temperature. By combining these data inputs an isentropic evaluation of the power generated by the prototype can be conducted.

6.4.3 local wave climate and power density

As no sensors were deployed to record the sub sea pressure in the vicinity of the prototype an analysis of this data has not been possible. However, existing mathematical modelling of the motion of the prototype with reference to specific waves can be used in conjunction with the hydrodynamic data to estimate the waves necessary to result in the motions recorded by the prototype.

The vertical displacement of the prototype is transferred into the frequency domain. Here the Response Amplitude Operator (RAO) of the prototype, at that specific frequency, is multiplied by the amplitude of the individual frequency components. This results in a plot of frequency against amplitude that has resulted in the recorded motion of the prototype. This method is presented in greater detail in section 7.

7.0 ANALYSIS OF THE PHYSICAL SEA TRIALS DATA RECORD

7.1 Introduction

The analysis of the sea trials data was conducted in order to validate the MOWC concept and estimate the overall conversion efficiency. The analysis was conducted in three main stages:

(iv) an initial analysis of the data to give primary indications for conversion efficiency and to assess the physical data for clarity and accuracy;
(v) an analysis of the local wave climate and wave power density during the sea trials;
(vi) an analysis of the internal power production.

The initial analysis utilised first principle equations to assess the power conversion of the turbine. This process was used to present an initial indication of the results in order to assess the physical data. The results of this analysis provided calibration information for the raw physical data and initial trends. However the methods used were simplistic in form, they will therefore not be presented within this report.

The analysis of the wave climate and calculation of the efficiency of the device were conducted using two independent equations and methods to ensure that the results of each method would be able to form an initial validation of the wave power density. The analysis of the local wave climate used the horizontal and vertical displacement of the prototype, in association with the RAO calculated for a simple spar. Analysis of the power conversion incorporated the internal water surface elevation, and the internal and external air pressure and temperature.

7.2 Evaluation of the wave power density per unit width incident upon the prototype

7.2.1 Aim

To calculate the mean wave power per unit width incident to the prototype during each sample period and the discussion of possible environmental effects on the analysis results.

7.2.2 Process of analysis:

Two methods were used to calculate the mean wave power density per unit width incident on the prototype device during each of the 20 minute sample periods. The first method (method A) utilises a standard wave power equation. The irregular input waveform is converted from the time to the frequency domain to identify the individual spectral components for frequency and amplitude, that make up the irregular wave form.

The second method (method B) also uses the spectral components, but these are used to calculate the zero moment of the wave spectrum and to identify the underlying dominant wave period. These components are then used to calculate the mean wave power density per unit width using the total energy period equation.

7.2.2.1 Method A

The heave motion of the prototype is converted into the incident waveform required to cause the resultant heave motion of the prototype. The prototype's heave motion was converted from the time domain to the frequency domain by means of a Fourier transform. Here the amplitude of the individual wave frequencies was combined with the heave response component for the prototype. The data was also filtered to remove the extremely long wave periods (100 > seconds), reducing the irregular wave form to the still water datum.

This calibrated input frequency spectrum can then be used to assess the wave power per unit width using a standard wave power equation [2].

$$P = \rho g^2 a^2 / 8\pi f \qquad (10)$$

Equation 10 calculates the power for each of the individual spectrum components; the mean of these components constitutes the mean power density per unit width incident on the prototype during the sample period.

The data shown in figure 7.1 was used as an input for a MATLAB based program to convert the time series data into a frequency spectral plot by means of a Fast Fourier Transform (FFT).

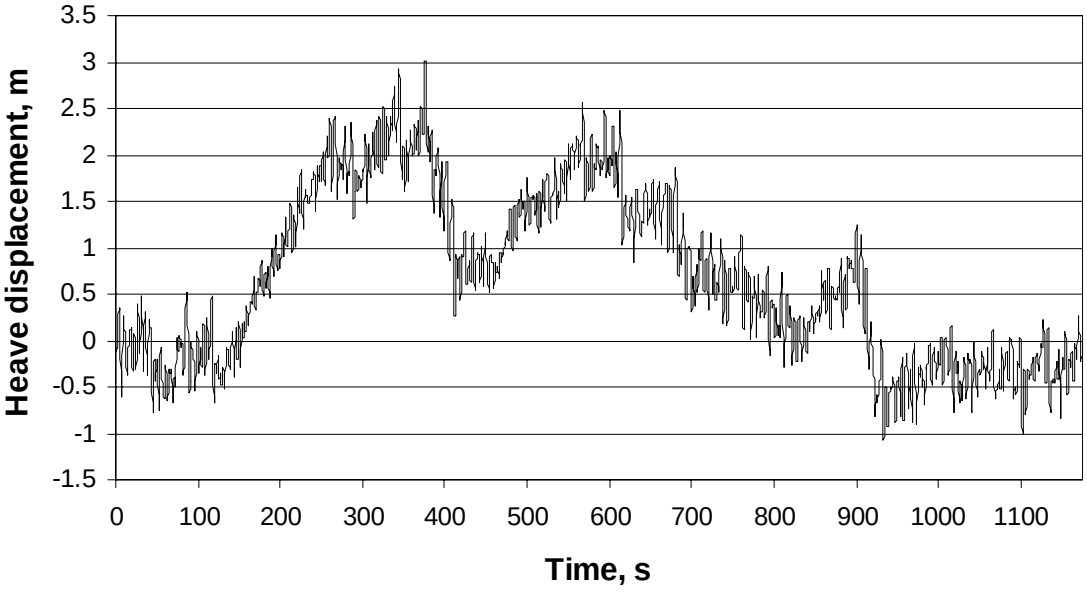

Figure 7.1, prototype heave displacement, between 0003 - 0023 on the 28th January 2002

The data is then multiplied by a value for the response heave component that corresponds to the associated frequency, see section 6, figure 7.2.

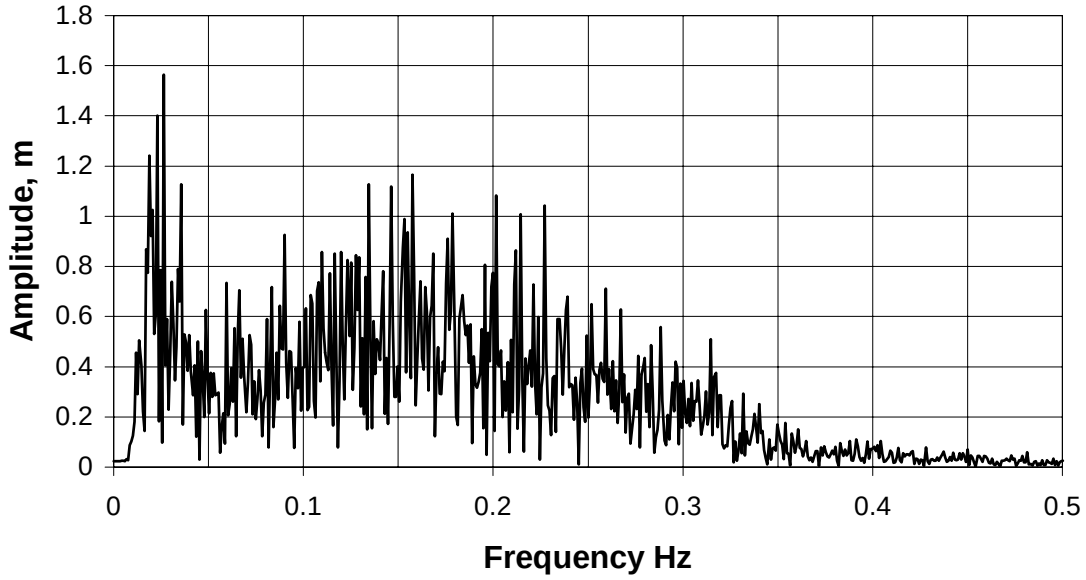

Figure 7.2, spectral plot showing the individual components of the input wave climate

This spectral data is then used in conjunction with the wave power per unit width equation 10, as input for the two unknowns, amplitude and frequency. This produces a value for the wave power density of each frequency component. The mean of these values represents the mean power generated during the 20 minute sample period, figure 7.3.

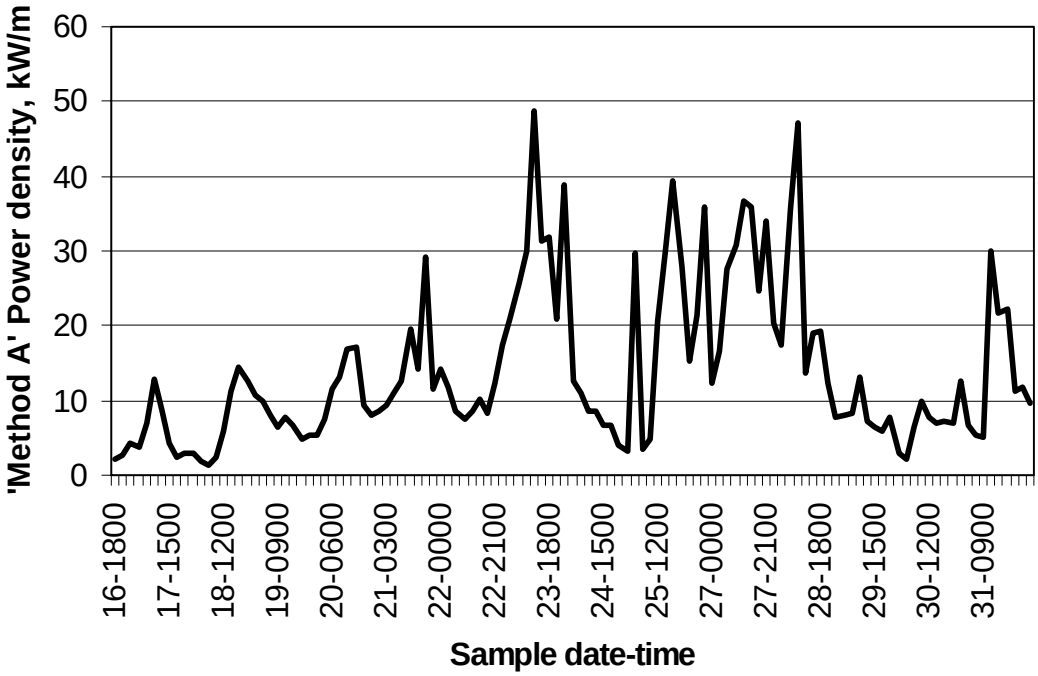

Figure 7.3, the mean power per unit width, incident on the prototype, calculated in the frequency domain using a standard wave power equation

7.2.2.2 Method B

By means of self-validation an alternative method using the total energy period equation, equation 11, was also used [2].

$$P = \rho g^2 / 4\pi T_E m_o \qquad (11)$$

This method assumes that there is an underlying dominant wave period present during any sample period that is responsible for the generation of a substantial proportion of the total wave power available for conversion during a specific sample period. By neglecting the other frequency components that make up the irregular waveform for the sample period, the total energy period equation calculated the mean wave power per unit width present during the sample period.

The equation requires the calculation of the mean square of the spectral moments contained within the irregular input waveform. The spectral moment is calculated in the frequency domain using the data shown in figure 7.3. The identification of the dominant wave period within the irregular waveform was then calculated by means of a cumulative method and visual interpretation.

These dominant frequency components were then used in conjunction with the spectral moments to calculate the mean wave power for the sample period, figure 7.4 and 7.5.

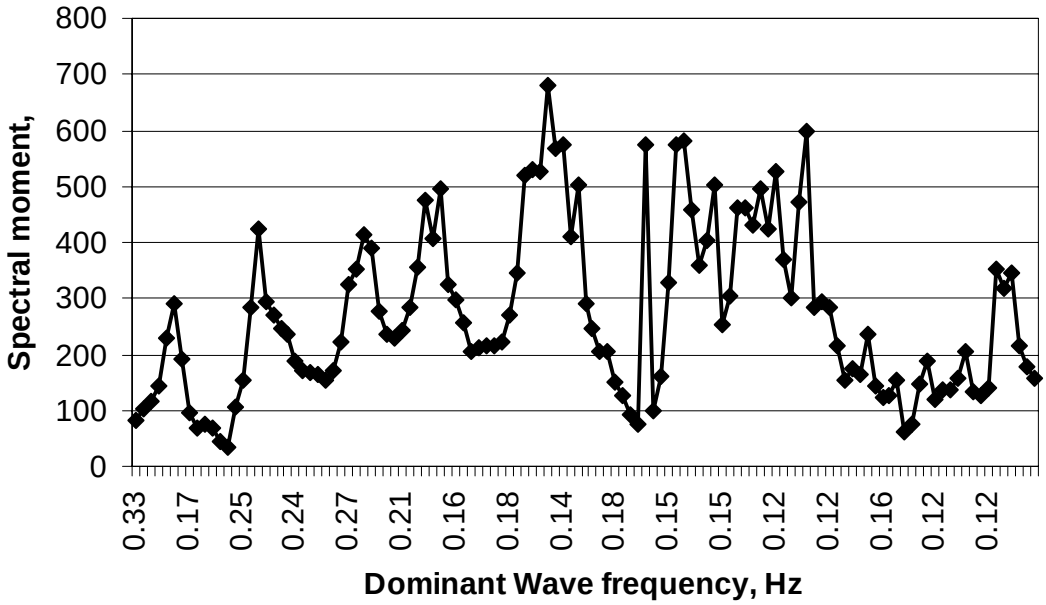

Figure 7.4, dominant wave frequency plotted against the corresponding spectral moment for each sample period

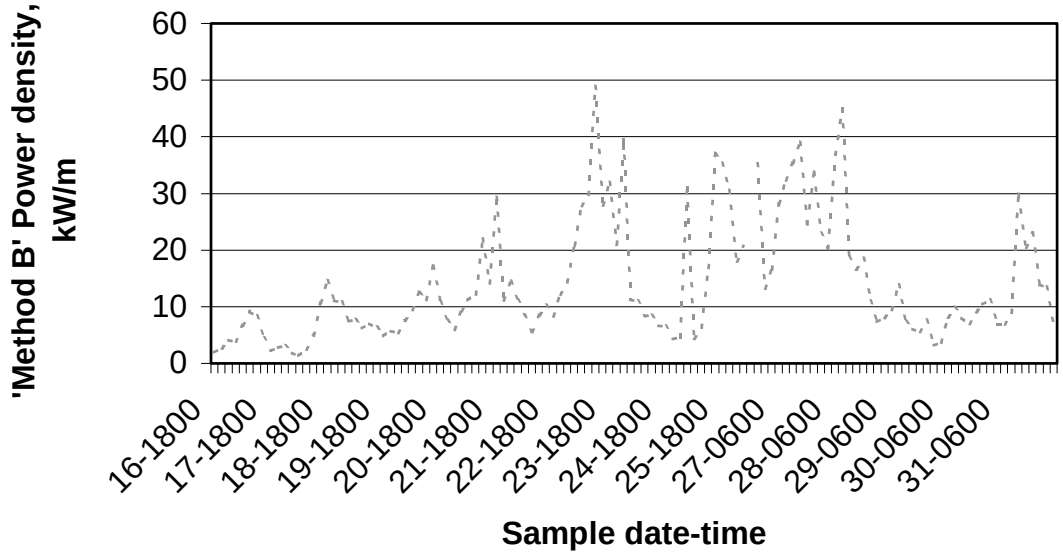

Figure 7.5, the mean wave power present during each sample period per unit width

The two output data sets were then compared to assess the ability of each method, figure 7.6.

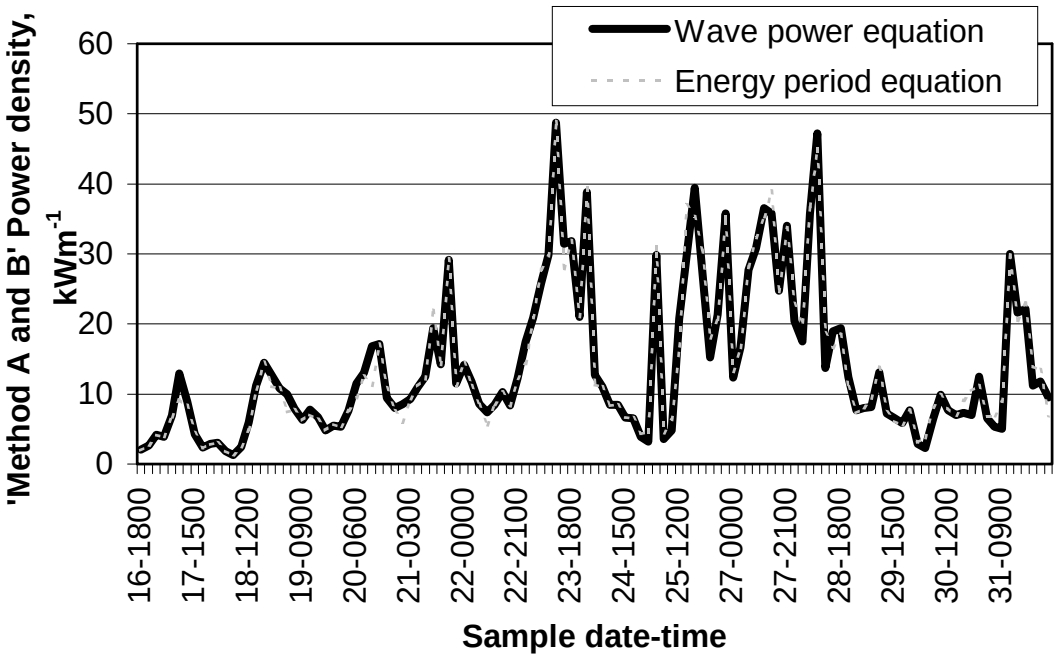

Figure 7.6, the plot shows the results generated by the two methods to calculate the mean wave power incident on the prototype during each sample period

7.3 Discussion of the incident wave power calculation

Each method used an independent equation for the calculation of the mean wave power incident on the prototype during each of the 20 minute sample periods. The only area where each of the methods possesses similarities is the use of the irregular input wave form being converted into its spectral components within the frequency domain. The method of this conversion utilises standard MATLAB algorithms for FFTs and wavelet calculations.

The calculation of the mean wave power in both method A and B, assumes that the spectral components are monochromatic wave forms in deep water [1]. As the device was located within 2 miles of the coast and in a relatively shallow water depth, it would be acceptable to see a reduction in the mean total wave power generated as a storm intensifies, this is seen during the deployment period.

As this process occurs the waves approaching the device build in height, becoming unstable due to the shallow water and break before reaching the prototype. However this breaking and resultant steepening of the incident waves can be neglected as the prototype records the actual input wave in the form of the heave motion.

Evidence of this effect can be seen by consideration of the local climatic wind speed and maximum gusts, figure 7.7.

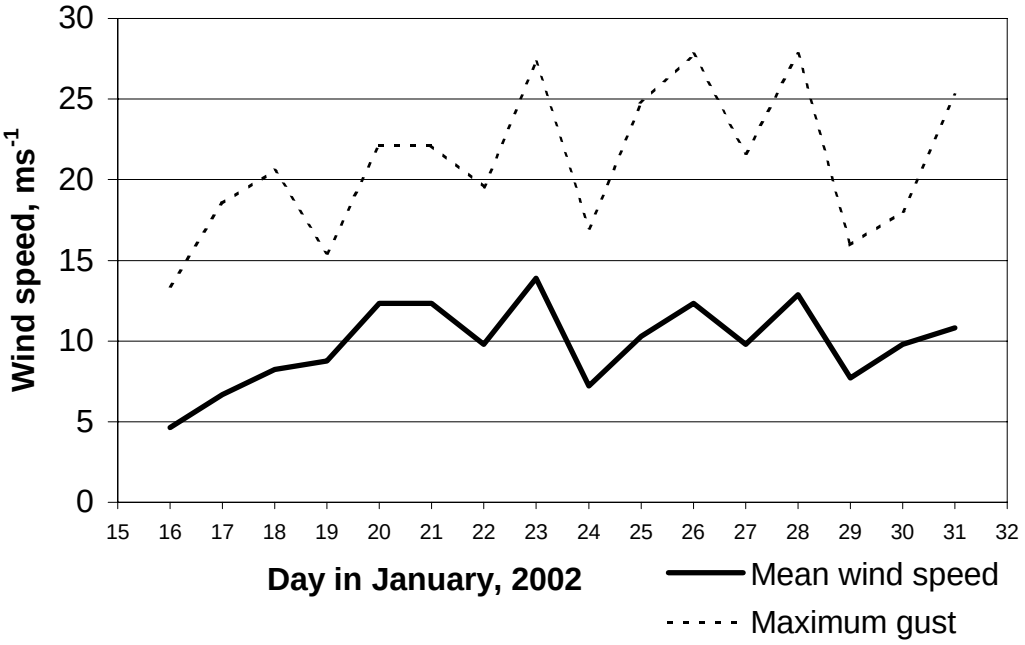

Figure 7.7, this graph shows the meteorological observations of the daily mean wind speed and the maximum gust recorded in Plymouth during January 2002

This graph shows that the weather during the sea trials period did not reduce in intensity as suggested by the graphs of incident wave power, but continued to develop into a fully developed storm. Therefore it can be concluded that the reduction in the incident wave power was due to environmental and physical factors, however the data was recorded by the prototype and will therefore show a fair representation of the power available for conversion as the test site.

The other area where errors may have been introduced is within the accelerometer data due to the motion of the device being used to calculate the input wave form. However this has already been discussed and it has been shown that this error will be minimal due to the design of the prototype and it's hydrodynamic properties, i.e. the prototype follows the water surface for wave periods above 3.5 seconds and does not appear to pitch and roll to a great extent.

The level of concurrence between the two methods of calculation, as shown in figure 7.6, gives the data a high degree of validation; the correlation between the two data sets has been calculated at 0.987. This level of correlation is encouraging and supports the use of this data in calculating the mean power available for conversion incident upon the prototype during each 20 minute sample period.

The calculation of the mean wave power density per unit width incident on the prototype during each 20 minute sample period was conducted using two independent equations within method A and B. These methods showed a high degree of correlation, 0.987, between the two methods. An average of the results generated by these two methods will then be used as the incident wave power density per unit width, figure 7.8.

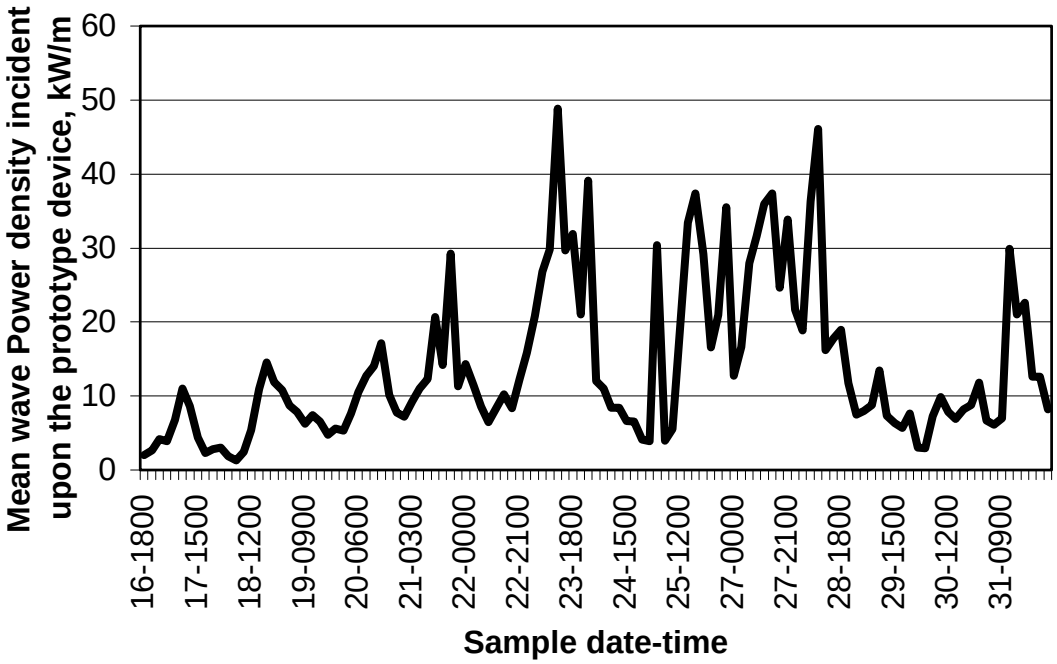

Figure 7.8, mean wave power per unit width incident on the prototype during each sample period

Using this mean incident wave power per unit width, an assessment can also be conducted for the increase in wave power corresponding to an increase in the dominant wave period, figure 7.9.

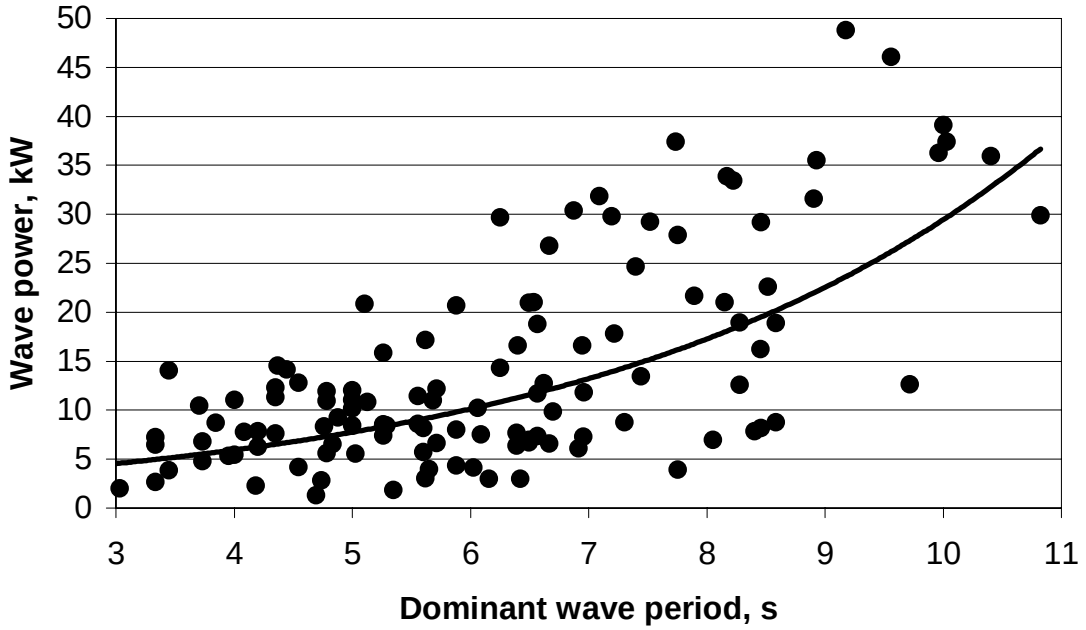

Figure 7.9, shows a linear trend of the increased wave power corresponding to the increasing length of the dominant wave period

This graph shows a reasonable exponential trend expected for the increase in incident wave power density per unit width, in relation to the progressive increase in the dominant wave period within each irregular wave climate.

7.4 Prototype conversion efficiency

The power generated by the prototype can be considered to have three stages of conversion:

(i) partial conversion of forward velocity of the wave motion and internal orbital motion of the water particle, into a vertical motion of an entrained water surface within the individual columns;

(ii) the conversion of an oscillating airflow into a rotational force generated by a self rectifying air turbine;

(iii) the conversion of the rotational force generated by the turbine into electrical power;

However, the data analysis only considered the efficiency of the overall prototype not the efficiency of the individual stages that are contained within the prototype. This method of analysis resulted in the evaluation of the prototype concept with regard to its ability to convert the incident wave power into an alternative form of power.

7.4.1 Isentropic method in principle

The thermodynamic flow through the turbine may be considered being a typical isentropic process. The flow within the device is assumed to be reversible enabling an ideal comparison between the internal process and the end states. As the air passes from the internal volume to the atmosphere its thermodynamic properties change as in a quasi-steady flow process. Since the process is assumed to be reversible and adiabatic, $pv^{\gamma} = \text{constant}$

An Isentropic flow process is given as:

$$W = \dot{m}\left\{C_p\left(T_2 - T_1\right) + \left(\frac{C_2^2 - C_1^2}{2000}\right)\right\} \qquad (12)$$

and:

$$\frac{T_2}{T_1} = \left(\frac{p_2}{p_1}\right)^{\frac{\gamma-1}{\gamma}} \quad \text{i.e. } T_2 = T_1\left(\frac{p_2}{p_1}\right)^{\frac{\gamma-1}{\gamma}} \qquad (13)$$

assuming kinetic energy terms are negligible, gives:

$$W = \dot{m} C_p T_1 \left(1 - \left(\frac{p_2}{p_1} \right)^{\frac{\gamma-1}{\gamma}} \right) \qquad (14)$$

Mass flow rate equation:

$$\dot{m} = C_d A_o p_1 \sqrt{\left(\frac{2\gamma}{\gamma-1} \right) \frac{1}{RT_1} \left[\left(\frac{p_2}{p_1} \right)^{\frac{2}{\gamma}} - \left(\frac{p_2}{p_1} \right)^{\frac{\gamma+1}{\gamma}} \right]} \qquad (15)$$

The mass flow rate equation assumes a perfect gas relationship during the reversible process with the identification of the orifice area and the dampening coefficient generated by the throttling effect of the turbine.

7.4.2 Method of Analysis

The analysis method uses the internal and external data generated by the prototype and associated evaluation. This data included:

(i)	internal air pressure;	- Physical data
(ii)	internal air temperature;	- Physical data
(iii)	atmospheric air pressure;	- Physical data
(iv)	atmospheric air temperature;	- Physical data
(v)	area of the exhaust orifice;	- Calculated
(vi)	discharge co-efficient;	- Calculated

The data was first calibrated and referenced to a datum level that enabled the direct comparison of each sensor. This calibration was also conducted between each sample period to ensure that a direct comparison during the sea trials period would be valid.

7.5 Results

Calculations were conducted independently for each of the three oscillating columns and for each of the 20 minute sample periods. These calculations resulted in computation of the mass flow rates and the power generated across the turbine.

The power produced by each of the individual columns was then added to produce a power generation by the entire system. By conducting individual calculations for each oscillating column, a comparison of the power generation compared to the dominant wave period and the other oscillating water columns is possible.

Calculation of the wave power density per unit width showed an increase in the activity of the wave power incident upon the prototype during the sea trials period, hence two sample periods representing a low and high wave power climate were used to compare the internal motions of the system and the specific power being generated at each sample point. The sample periods used were recorded at 12:00 on the 18thand 23rd January 2002.

The explicit power generated at each of the sample points within each of the 20 minute sample periods shows the variations of the power produced. This depicts the level of variation in the power generated by each individual column, which is reduced through the combination of multiple columns, figure 7.10 and 7.11, the isentropic power generated by the individual columns are included in Appendix B.

The power generated by the individual columns shows that there is very little interaction between the water surface motions within the individual columns. This concludes that there is no phase locking evident between the individual columns as the airflows are combined within a single air turbine.

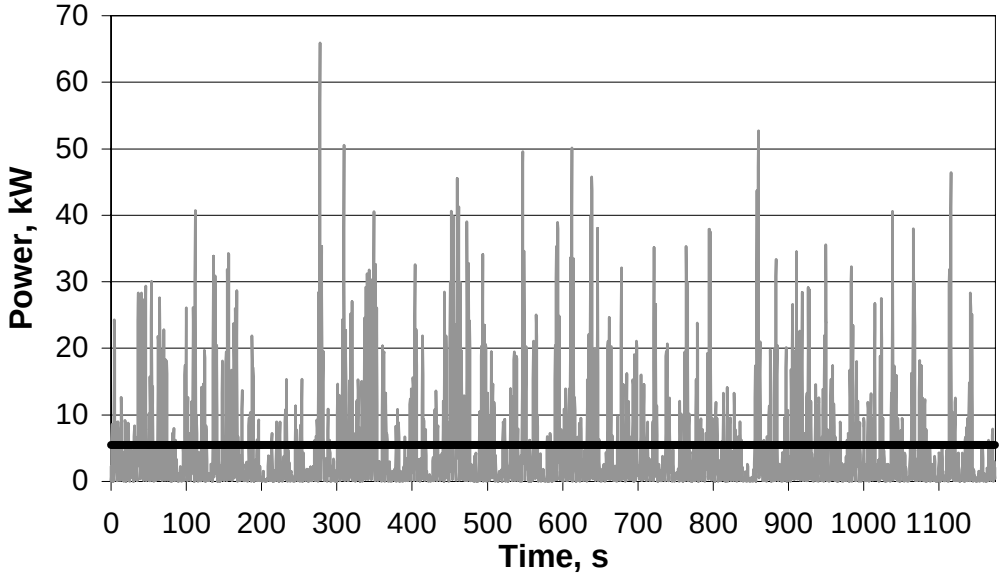

Figure 7.10, power generated the prototype between 1203 and 1223 on the 18th January 2002. The mean power generated was 5.46 kW.

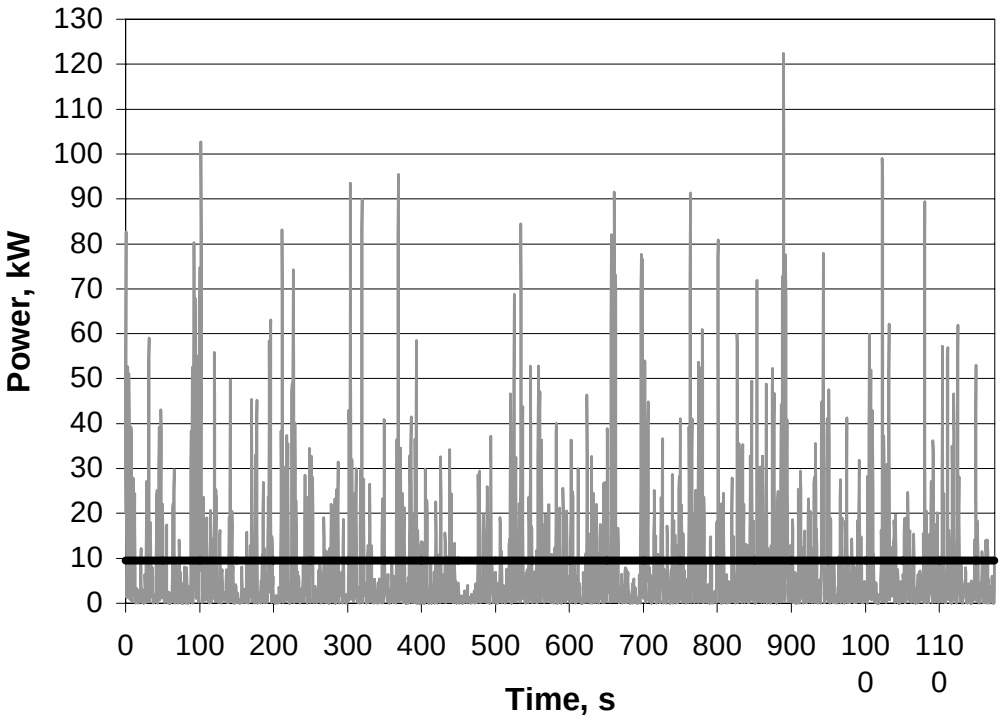

Figure 7.11, power generated the prototype between 1203 and 1223 on the 23rd January 2002. The mean power generated was 9.43 kW

The results calculated for the isentropic power generation shows a high level of peak power generation, this effect is predominantly due to the method used to calculate the power at each

sample point. The actual power generated by the electrical generator would not experience such high levels of variation, as the turbine and generator would retain some kinetic energy in the form of momentum as the airflows change.

The effect of this stored energy within this system would depend upon the entrained inertia within the overall turbine rotor and generator. By accurately matching the turbine and generator with regards to their associated mass, the level of variation can be minimised.

The individual columns also show peak power activity over short periods of time, this short instantaneous power generation shows a rapid rise in the displacement of the internal water surface and air pressure. Again the extent of these relatively short pulses in the power generation would be reduced as the multiple columns combine within the turbine and these fluctuations are reduced as they are converted to mechanical action within the turbine and drive train.

In order to assess the efficiency and potential of the prototype in converting wave power to electrical energy, the assessment is concerned with the overall efficiency of the prototype during the entire sea trial period. This assessment compares the mean power generated by the prototype during each 20 minute sample period with the dominant wave period and mean wave power incident on the prototype.

7.6 Evaluation of conversion efficiency and dominant wave period

The dominant wave periods present during the 20 minute sample periods represent the underlying natural period of the input wave form. The data plotted in figure 7.12 showed the overall ability of the prototype to convert the incident wave power into electrical energy. Only columns 1 and 3 are shown for clarity.

The graph shows that the mean power generated varied over the period of the sea trials and slowly fluctuated between the shorter and longer column.

Column 1 with a draught of 4m generates within a range of 0 – 4 kW. As the dominant wave periods increase the level of power generated by the column is reduced. It continues to generate within this power band, but as the dominant wave periods increase the power generated is less dominant than that being generated by the longer 7m draught column 3.

The low values for R^2 given for each column power generation show a highly erratic fluctuation in the mean power produced by each of the columns. This effect is directly related to the erratic nature of the input wave climate.

For short dominant wave periods the longer 7m draught column contributes less than that of the 4m column to the overall power generation. However, as the dominant wave periods increase the contribution made by the longer 7m column is also increased, until it is generating a substantially greater amount of power than the shorter 4m column. This relationship and its effect on the overall power generation is shown in figure 7.13.

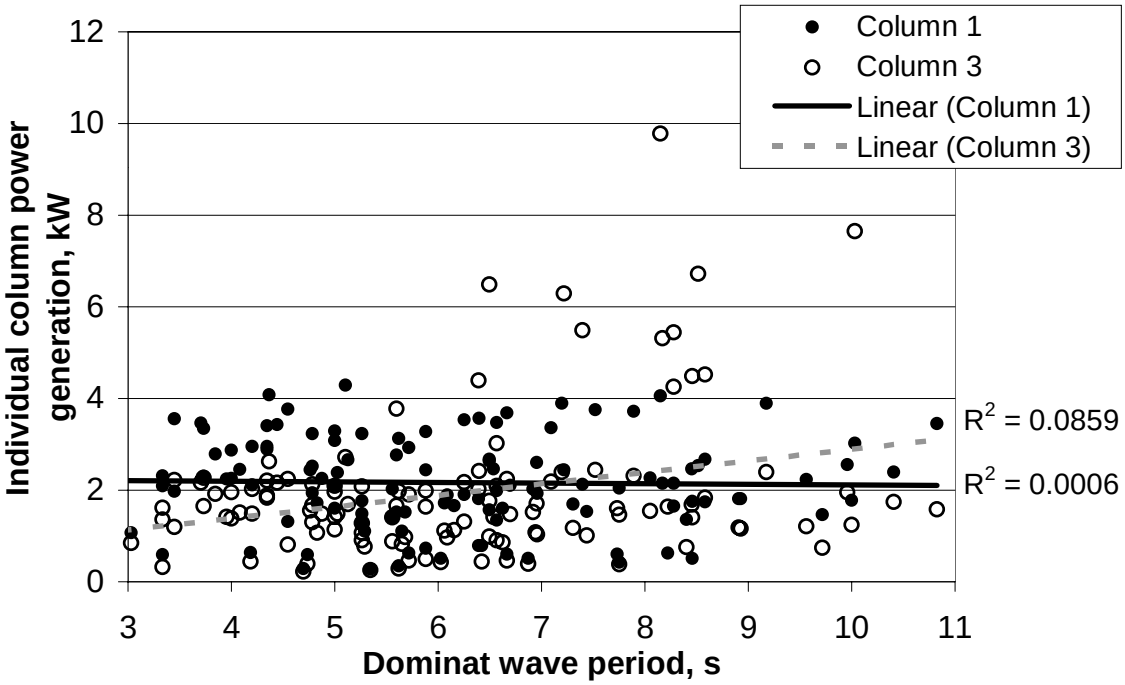

Figure 7.12, individual power generated by column 1 and 3 plotted against dominant wave period

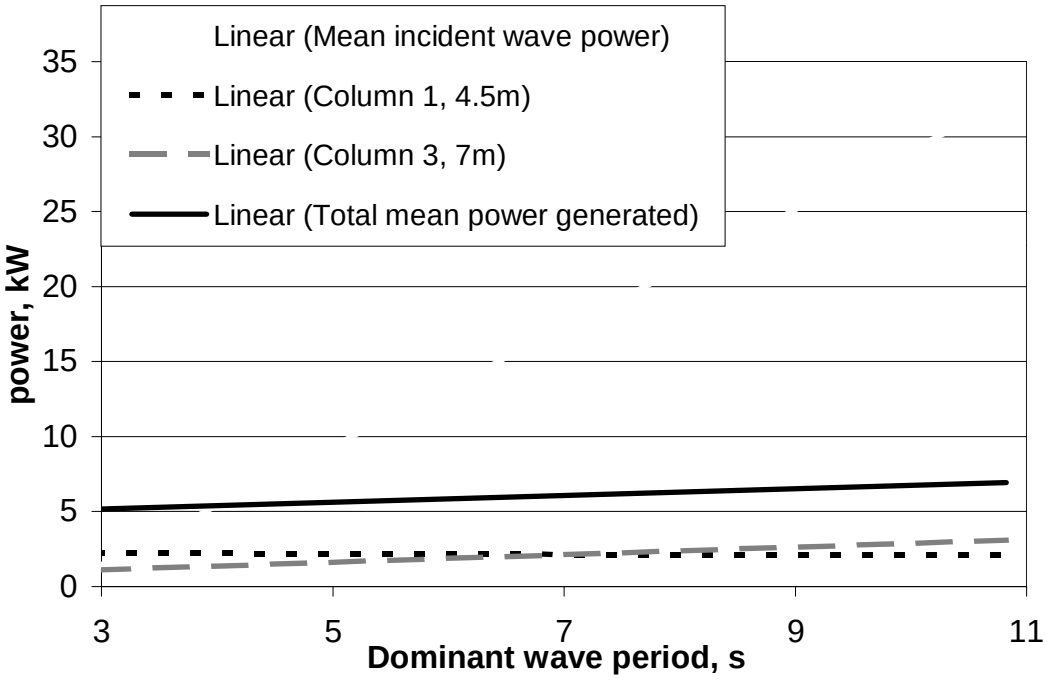

Figure 7.13, the linear trend lines for the incident wave power, power generated by column 1 and 3, and the total mean power generated by the prototype

The graph shows the increase in incident wave power density per unit width as the dominant wave period increases, it also shows the relative increase and decrease in the power generated by the individual oscillating columns. The increase in the total power produced by the device as the dominant wave period increases is shown in black. What is most noticeable is the relatively low rise in power generation by the prototype as the incident wave power increases due to longer dominant wave periods.

This effect is a direct result of the incorporation of the multiple oscillating columns, at shorter wave periods power is generated by the shorter draught columns, as the wave climate changes so too does the contributions made by the additional oscillating columns. The overall effect of this increase and decreasing level of contribution made by the individual columns creates this semi-self regulating system, promoting a greater stability of electrical power being generated by the device.

7.7 Discussion of the prototype conversion efficiency

In order to assess the overall power efficiency of the device two components were identified:

(i) the wave power incident on the prototype;
(ii) the power produced across the turbine;

The wave power density per unit width incident on the device was discussed within section 7.2. Figure 7.8 shows the mean wave power density per unit width present in a specific width of wave front. For a shore based oscillating water column it is relatively simple to multiply the power per unit width by the capture width of the device to generate a figure for the total power incident upon the device.

One of the many features of the multiple oscillating water column device is its presentation of a small aspect to the oncoming waves. This small aspect reduces the forces placed on the device by the incident waves, it would also reduce the incident wave power acting on the device, as the value of the wave power is considered over a specific width of wave frontage, i.e. the smaller the device the less power it will experience therefore the less power it will produce. While this statement is not wholly inaccurate, the level of power produced by a point absorbing device such as the MOWC may be greater than that said to be present using the widely accepted wave power per unit width equation.

Using the wave power per unit width equation, eqn. 10, to assess the wave power incident upon the prototype requires the capture width of the prototype be identified. As the device was free floating the capture width will consist of several sub components:

(i)	waterline length;	- 4m
(ii)	cross sectional width of the waterplane;	- 1m
(iii)	diameter of the oscillating columns;	- 0.5m
(iv)	orientation of the oscillating water columns	-
(v)	number of oscillating columns	- 3
(vi)	prototype displacement	- 12,500 kg’s
(vii)	hydrodynamic motion of the prototype	-

The level of influence each of these sub components has on the overall capture width of the prototype will vary directly between each component and will vary marginally as the prototype heaves in the sea way. As the prototype was allowed to move freely in heave, the largest component will be the cross sectional area and waterline area of the device.

By allowing the prototype to heave the generation potential of the columns was greatly reduced, the device uses pressure fluctuations across the base of the columns to force water up the columns as a wave peak approaches and fall as the wave peak recedes. The level of power reduction can be assessed through a comparison of the instantaneous prototype heave and the displacement of the internal water surface within each of the columns, with regard to the potential pressure fluctuation across the base of the column. The greater the vertical heave displacement, the greater the reduction of the pressure fluctuation across the base of the column.

For a fixed device, i.e. one that is restricted in heave, the waterline length and waterplane cross sectional width will not affect the capture width of the device. The only components will be the number of oscillating columns, the diameter of these columns and their orientation. Within the prototype the number, diameter and orientation of the oscillating columns was responsible for the power generated not the capture of the incident wave power.

Therefore the capture width of the prototype will be a product of the prototypes waterplane cross sectional width and the number and diameter of the oscillating columns, i.e. between 4.4m and 0.5m x 3 (waterline length, diameter of the columns, number of the columns). However, at the waterplane the prototypes cross sectional width consists of an annulus floatation collar that reduces its actual cross sectional width to 1.0m.

The incident wave field acted upon the prototype over the full width of the waterplane, however the incident wave was converted within the confines of three oscillating columns. The actual power incident upon the prototype can therefore be said to act on the device over a width of approximately 1.5m for the purpose of this comparative assessment.

The multiplication of the incident wave power per unit width by this capture width will then give the wave power available for conversion by the prototype, figure 7.14.

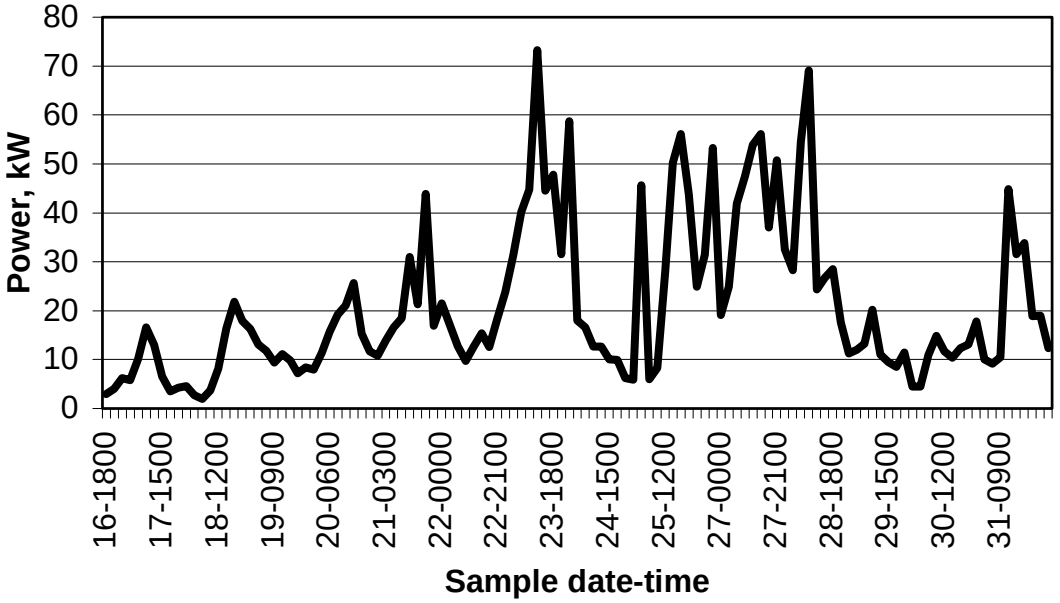

Figure 7.14, the mean wave power incident on the prototype during each 20 minute sample period available for conversion by the oscillating columns

The mean power produce by the prototype during each 20 minute sample period can then be compared to the incident wave power, figure 7.15, and an efficiency of the prototype calculated for each period sample, figure 7.16.

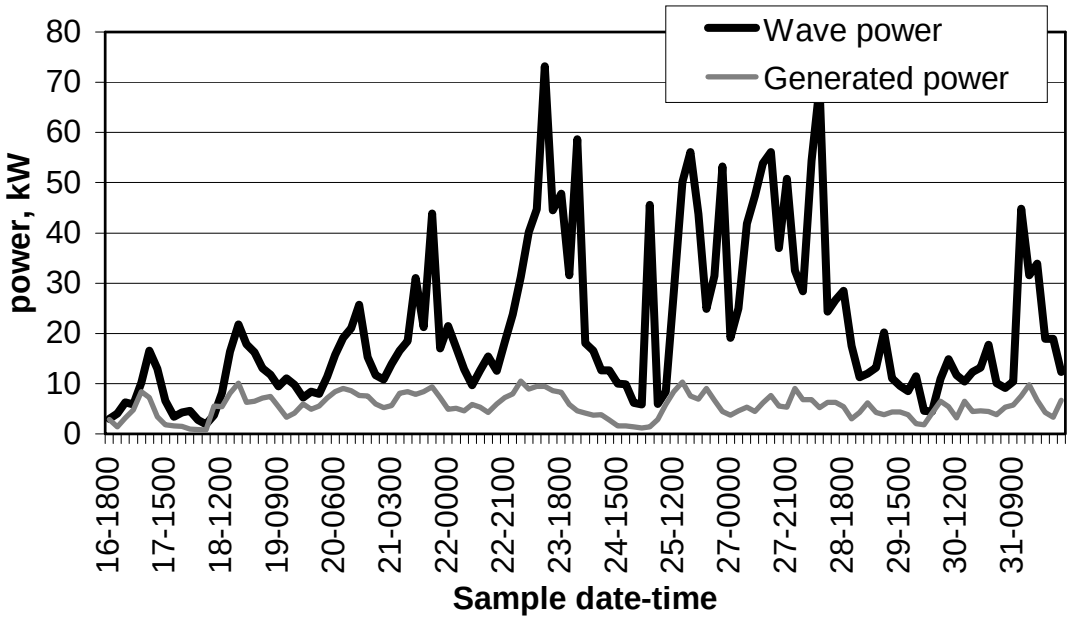

Figure 7.15, mean incident wave power and mean power generated by the prototype during each 20 minute sample period

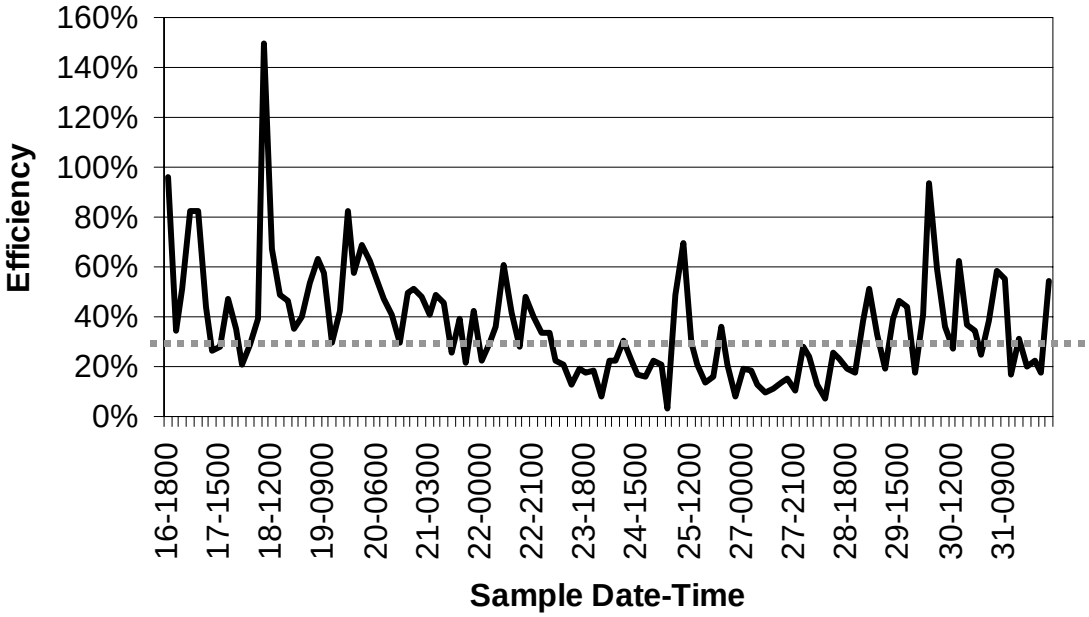

Figure 7.16, the conversion efficiency of the prototype during each 20 minute sample period and the mean efficiency of the prototype over the entire sea trials period, gray dotted line

The graph showing the incident wave power and the power generated by the prototype during each 20 minute sample period shows that the power generated by the prototype remains below 10kW regardless of the heightened level of incident wave power. The correlation between the incident wave power and the power generated by the prototype was calculated at 0.47. This shows a fair comparison between the two data records and again shows the ability of the device to self-regulate in high power sea states typical of storm periods.

The actual efficiency of the device during each 20 minute sample period was calculated by the direct comparison of each power value. Representation of the conversion efficiency of the prototype in this format is useful for marketing purposes. However for future development it is of greater use to plot the conversion efficiency of the prototype and individual columns with reference to the dominant wave period within each irregular input wave field, figure 7.17.

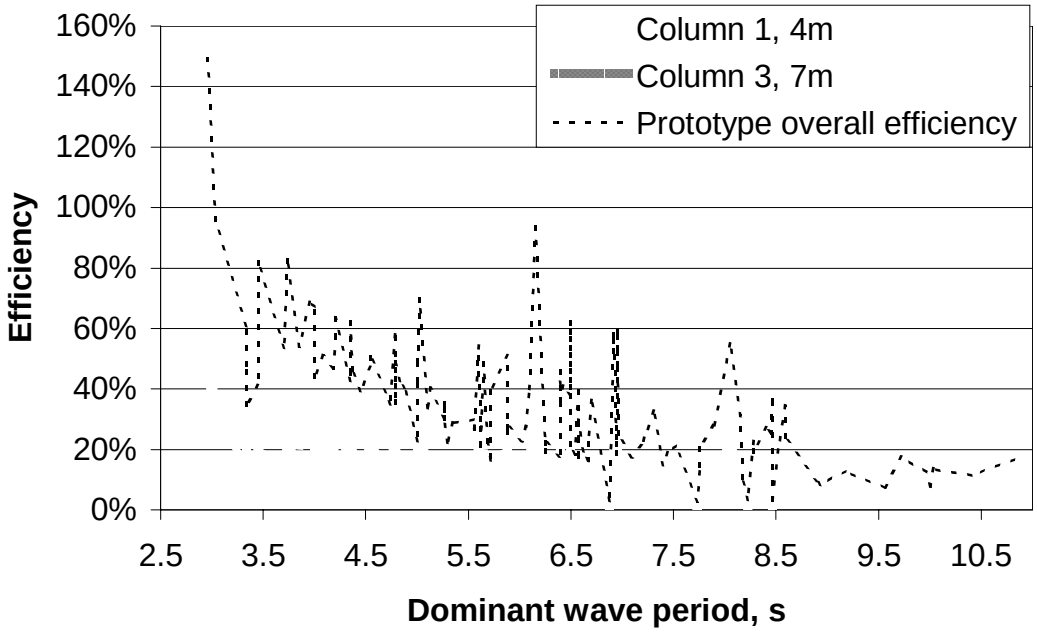

Figure 7.17, individual column and prototype overall efficiency plotted against dominant wave period

The graph shows that the prototype had greater conversion efficiency during wave climates that had short underlying dominant wave periods. As previously discussed the prototype was allowed to heave freely in order to reduce its power generation ability. This graph shows that in sea states where the hydrodynamic motion of the prototype is increased a greater level of power generation is achieved. This effect is confirmed in the analysis of the hydrodynamic motion of the device, for wave periods between 2.5 and 3.2 seconds an amplification of the prototypes heave motion can be expected.

As a result the sample periods that experienced short dominant wave periods could be neglected to remove results where the prototypes power generation may have been increased due to the prototypes' hydrodynamic motion, this includes only two sample points below 3.3 seconds.

It is also worth noting that the conversion efficiency of the shorter draught columns is almost always greater than the longer column, it is felt that this is due to the hydrodynamic motion of the prototype. The difference between the two column efficiencies is greatest at shorter wave periods; this would be expected as the longer column is affected greatest at longer wave periods.

The efficiency peak at 6 seconds indicates a possible resonance effect being generated, there are also peaks at 5, 6.5 and 7 seconds. Further analysis will be conducted to identify the grounds for these higher efficiencies, but preliminary results indicate potential resonance effects within the columns. However it is worth noting that the increase in efficiency at 6 seconds coincides with the mathematically predicted resonance within a 7m column at the same wave period.

With regard to the internal conversion efficiency of the initial prototype the evaluation of its ability was centered on the overall efficiency of the system and interaction of the individual oscillating columns. This evaluation was conducted with reference to the following:

(i) Did the individual oscillating columns show any signs of phase locking?
(ii) The prototype included a 5kW turbine and generator, did the prototype generate the level of power and what was the overall conversion efficiency?
(iii) The prototype was built to withstand the marine environment without much consideration the flow of air to and from the oscillating columns. Are there fundamental design alterations that would increase the conversion efficiency?

Initial studies, using elementary equations, were conducted to assess the physical data for accuracy and to identify the calibration required by each sensor. This initial analysis was simplistic in its approach but formed a fundamental stage in the assessment of the physical data. This assessment was also concerned with the interactions between the individual oscillating columns and their interaction through the air turbine.

It was hypothesized that the individual columns may interact to such an extent that they would begin to act in harmony with regard to their motion and the phase angle between each column. If phase locking took place then it would increase the instantaneous mass flow through the turbine when the columns exhaled and withdrew in relation to each other. If no phase locking took place between the individual columns, then the mass flow through the turbine would be equal to that if they were locked.

However, the mass flow from non-phase locked columns would be distributed more evenly over each cycle of up and down stroke. This effect reduces the operational range required of the turbine and increases the operational efficiency of the concept in converting irregular input wave energy into a continuous supply of electrical power.

An objective of the previous European CRAFT project was the measure through generation of the ability of the prototype to convert enough wave power to generate 5kW of electrical power. This ability was to be assessed by means of a self-rectifying turbine and electrical generator. This was to be recorded by means of a turbine shaft rotation speed and the measurement of the current produced by the generator.

Unfortunately both of these sensors failed to operate and the weather conditions at the test site prevented any remedial work being conducted. The assessment of the power generation of the prototype would then have to be conducted assuming thermodynamic processes within the prototype. The self-rectifying turbine used within the prototype was only designed to generate 5kW from the airflows generated. The assessment of the internal air pressures, temperatures and water surface levels assuming an isentropic process, indicate the level of power generated across the turbine.

The actual electrical power produced by the generator is unknown, however on inspection of the power dissipation system, heat elements secured below the waterline, the level of paint scorching indicated that the generator had produced a substantial amount of electrical power during the sea trial period.

The efficiency of the device can be calculated using several methods; the method used within this report compared the mean wave power incident upon the prototype during each of the 20 minute sample periods. This value has taken into account the capture width of the prototype and was calculated using two independent methods. As this data has been recorded from a real environment it shows real trends and the extent of the irregular nature of the marine environment.

However, as the heave of the prototype would reduce the pressure fluctuations across the base of the columns, so the motion of the heave motion of the prototype would also increase the power generated. In wave climates that correspond to an increased excitation of the prototype a greater level of power was evident. From evaluation of the hydrodynamic motion of the prototype it was seen that there was an increase in its excitation at wave periods between 2.5 and 3 seconds. In order to reduce the possible increase in conversion efficiency any sample period with a dominant wave period less than 3.5 seconds was neglected.

After the removal of the sample periods that showed contamination by the heave motion, those corresponding to a dominant wave period of less than 3 seconds, an overall efficiency for the conversion of the wave power across the turbine during the sea trial period was calculated at 34.49%, for a capture width of 1.5m. The final efficiency of the prototype would be slightly less than this after inclusion of the efficiency of the generator to convert the power generated across the turbine into electrical power.

8 CONCLUSIONS AND RECOMMENDATIONS

8.1 Introduction

Successful acquisition of the sea trials data was instrumental in accomplishing the project objective. The data recorded allowed the calculation of the conversion efficiency of the prototype during the sea trials period and recommendations for future data analysis.

8.2 Wave climate characterisation

Evaluation of the wave power incident on the prototype during the sea trials period was conducted using existing equations. However the surface elevations recorded at the test site were not deduced as intended by a three dimensional sub sea pressure array. The motion of the prototype was used in conjunction with the heave response of the structure to the incident wave motions.

This method of processing allowed calculation of the time series surface elevations recorded during the sea trials period. Fourier transforms were used to assess the individual surface profiles and calculate a mean power per unit width incident on the prototype. Multiplication of this value with that of the capture width of the prototype resulted in the calculation of the mean power incident on the prototype available for conversion during the sample period, figure 8.1.

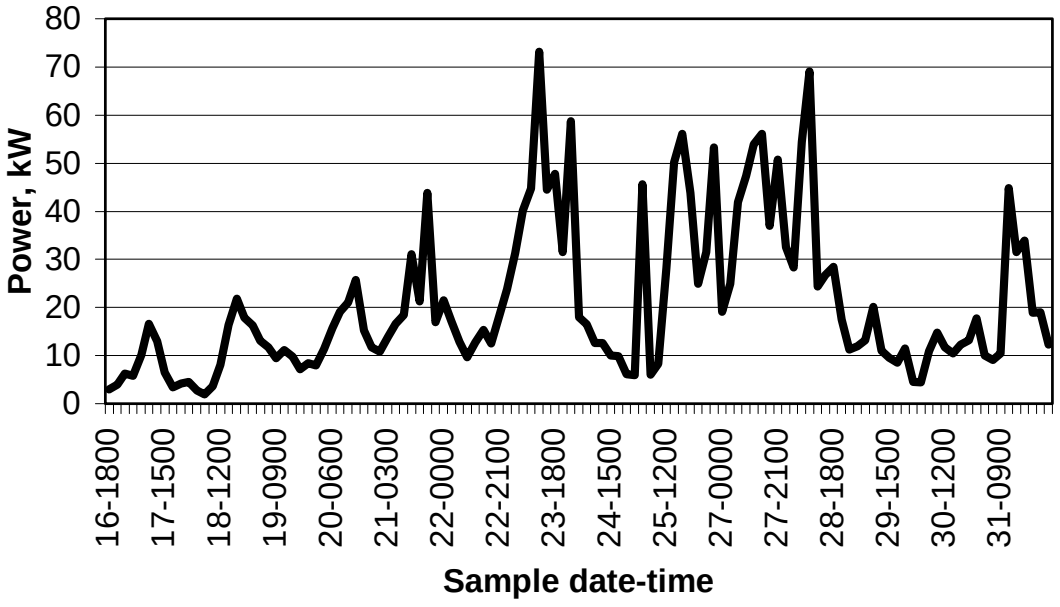

Figure 8.1, mean wave power available for conversion during each 20 minute sample period.

8.3 Conversion efficiency of the prototype during the sea trials

The efficiency of the prototype during the sea trials period was calculated using the physical data recorded assuming an isentropic process. The mean of the instantaneous power generated across the turbine was then calculated in order to compare the power generated with the power available for conversion, figure 8.2.

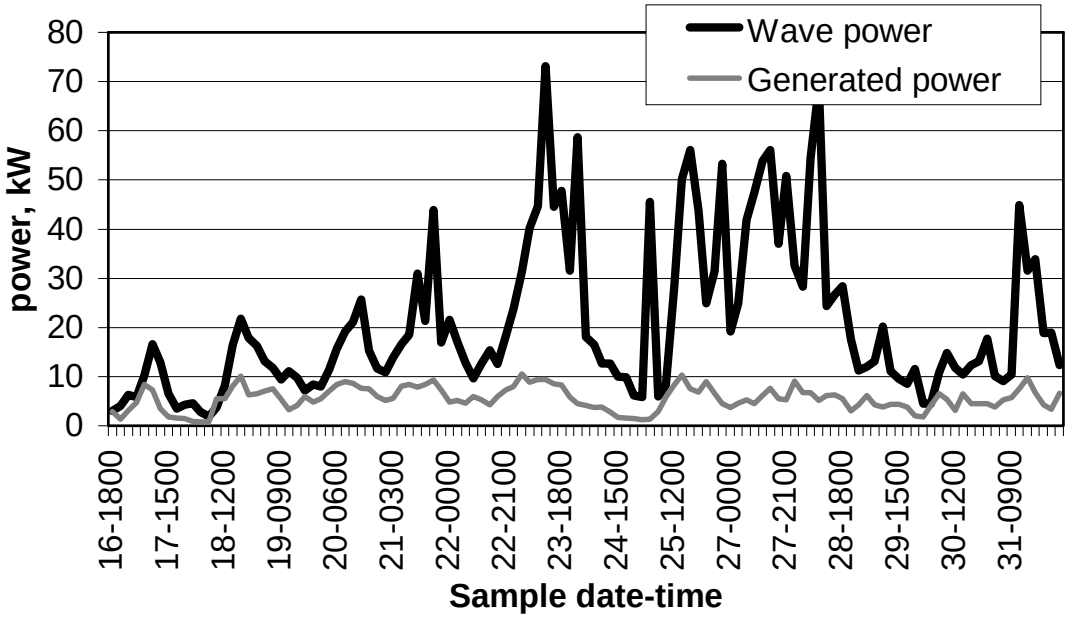

Figure 8.2, mean incident wave power and mean power generated by the prototype during each 20 minute sample period.

The overall conversion efficiency of the prototype during the sea trials was calculated at 34.5%. Conversion efficiency of over 100% was evident when the dominant input wave period was close to the natural resonant period of the prototype.

8.4 Recommendations

Further analysis of the sea trials data would allow the calculation of the power potential for a fixed device by subtracting the heave component from the analysis process. Calculating the generation potential for a fixed structure, would then allow calculation of the conversion efficiency for individual oscillating water column with regard to the dominant incident wave period.

Quantification of these parameters will permit the evaluation of a full size unit incorporating multiple columns with regard to the wave resource available at locations worldwide.

9 REFERENCES

1. European Union contract number JOR3-CT98-7026 final report.

2. Tucker.M.J., Pit.E.G., **Waves in Ocean Engineering**, Elsever Ocean Engineering Book, Series Volume 5, 2001, ISBN 0080435661.

3. Evans.D.V., **Power from sea waves**, Ann. Rev. Fluid. Mech., 13:157-87, 1981.

4. Maeda.H., Santhakumar.S., Setoguchi.T., Takao.M., Kinoue.Y., Keaneko.K., **Performance of an impulse turbine with fixed guide vanes for wave power conversion**. Renewable Energy, volume 17, 533-547, 1999

APPENDIX A

EXPLANATION OF HYDRODYNAMIC STABILITY

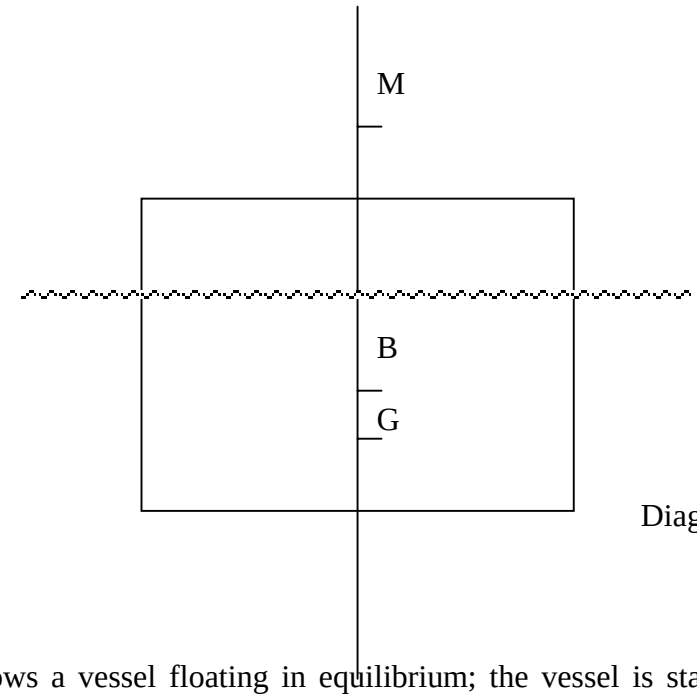

Diagram 1

Diagram 1 shows a vessel floating in equilibrium; the vessel is stable and upright. Should an external force be applied to the vessel, it will heel in response to this force with an associated movement of the centre of buoyancy to correspond with the centre of the submerged volume, diagram 2. The righting lever of the vessel will act between a vertical line suspended through the metacentre and the centre of gravity.

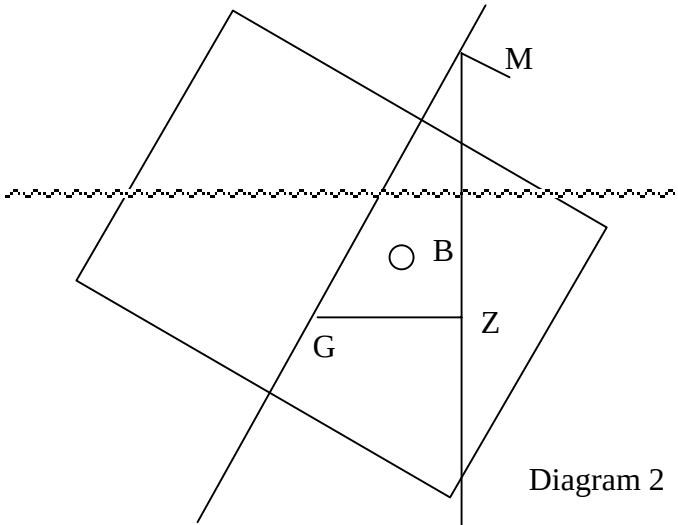

Diagram 2

Distance between GZ is the righting lever through which the vessel is resisting the heeling force, the greater the righting lever the greater the righting force and greater resistance a vessel has to heeling.

Vessel 1 **Vessel 2**

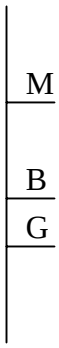

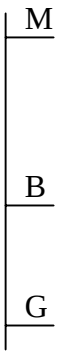

Vessel 1 Vessel 2

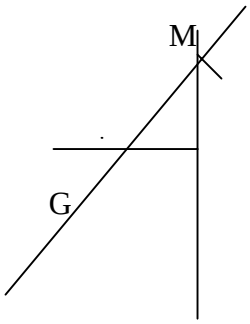

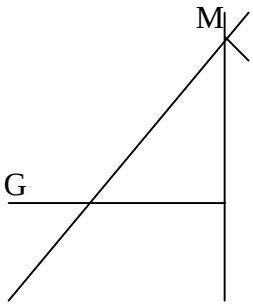

The righting lever of vessel 2 is greater than vessel 1. Vessel 2 is the said to be stiffer than vessel 1, possessing greater stability to resist roll and pitching.

APPENDIX B

INDIVIDUAL POWER GENERATION OF COLUMNS 1, 2, 3 AND THE TOTAL POWER GENERATED BETWEEN 1203 AND 1223 ON THE 18TH AND 23RD JANUARY 2002

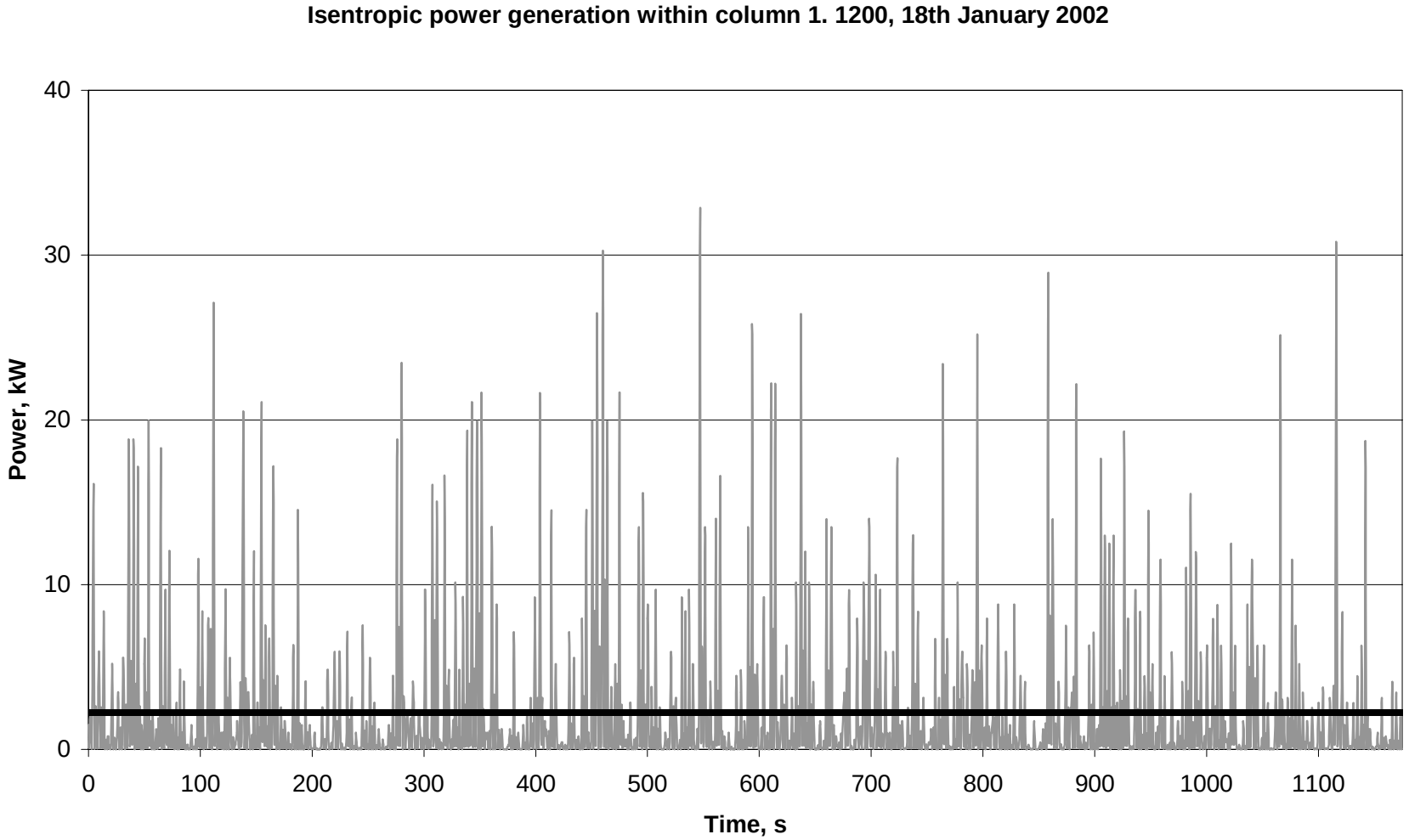
Isentropic power generation within column 1. 1200, 18th January 2002
Power, kW
40
30
20
10
0
0
100
200
300
400
500
600
700
800
900
1000
1100
Time, s

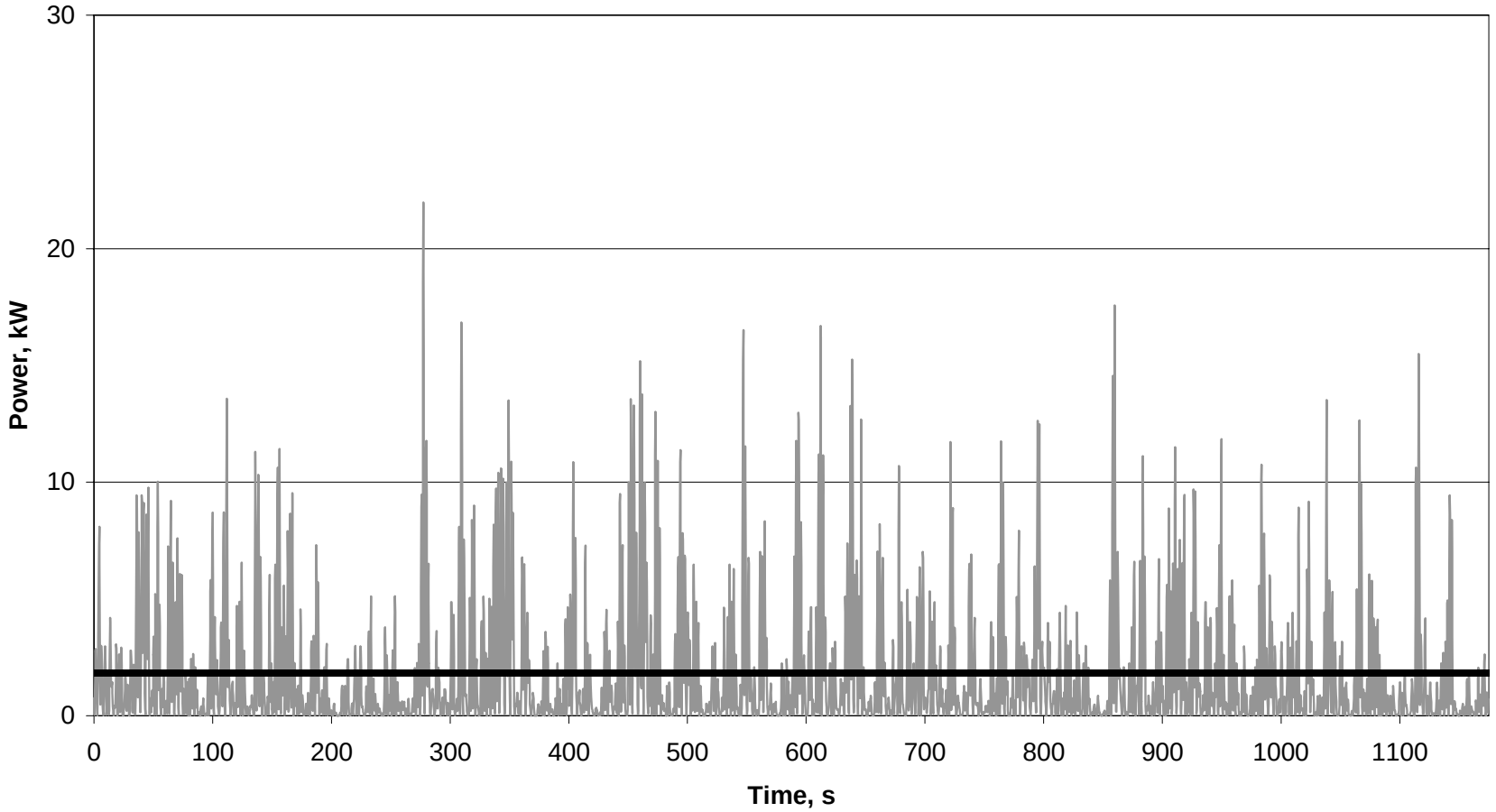
Isentropic power generation within column 2. 1200, 18th January 2002
Power, kW
30
20
10
0
0
100
200
300
400
500
600
700
800
900
1000
1100
Time, s

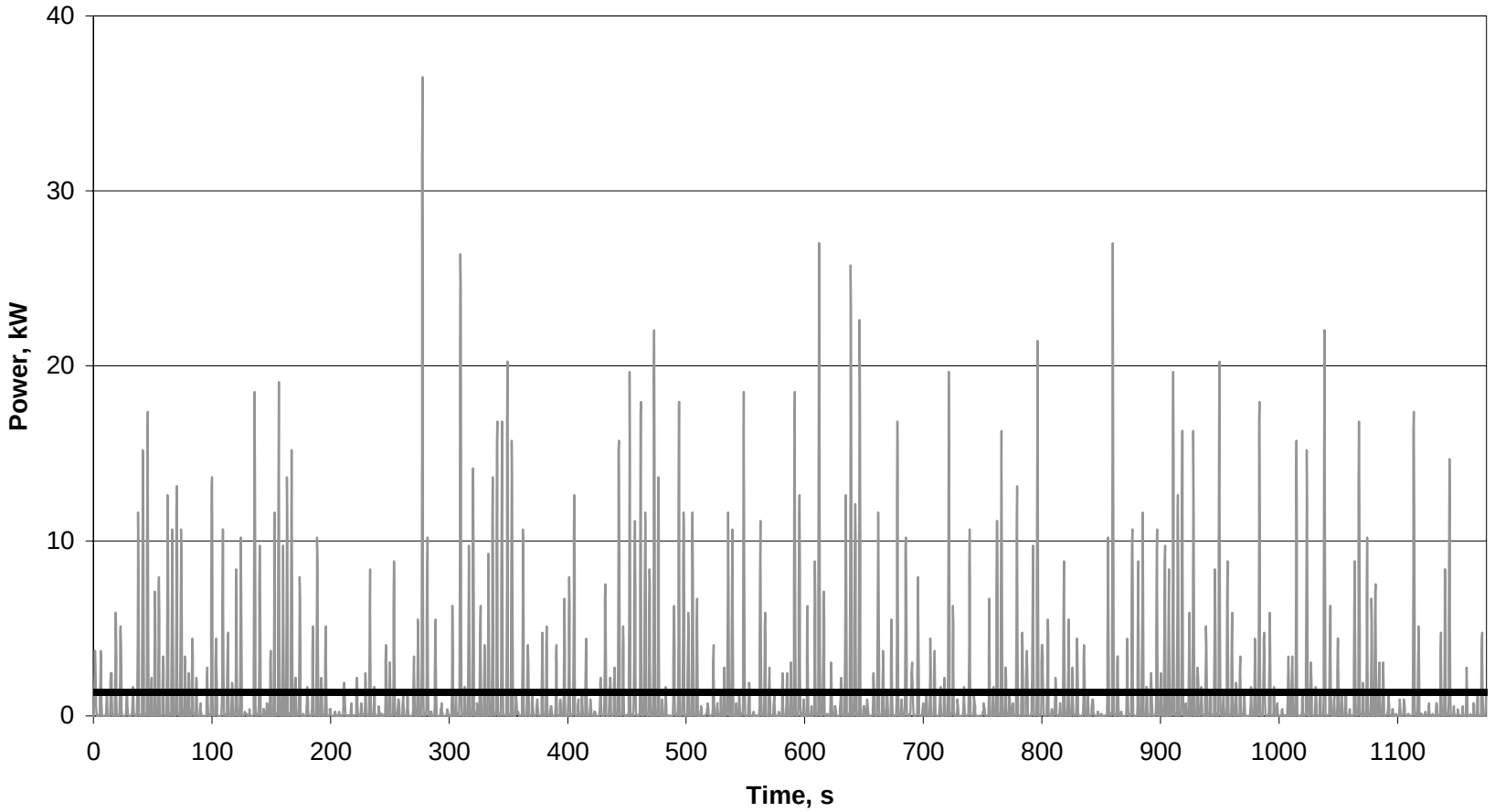
Isentropic power generation within column 3. 1200, 18th January 2002
Power, kW
40
30
20
10
0
0
100
200
300
400
500
600
700
800
900
1000
1100
Time, s

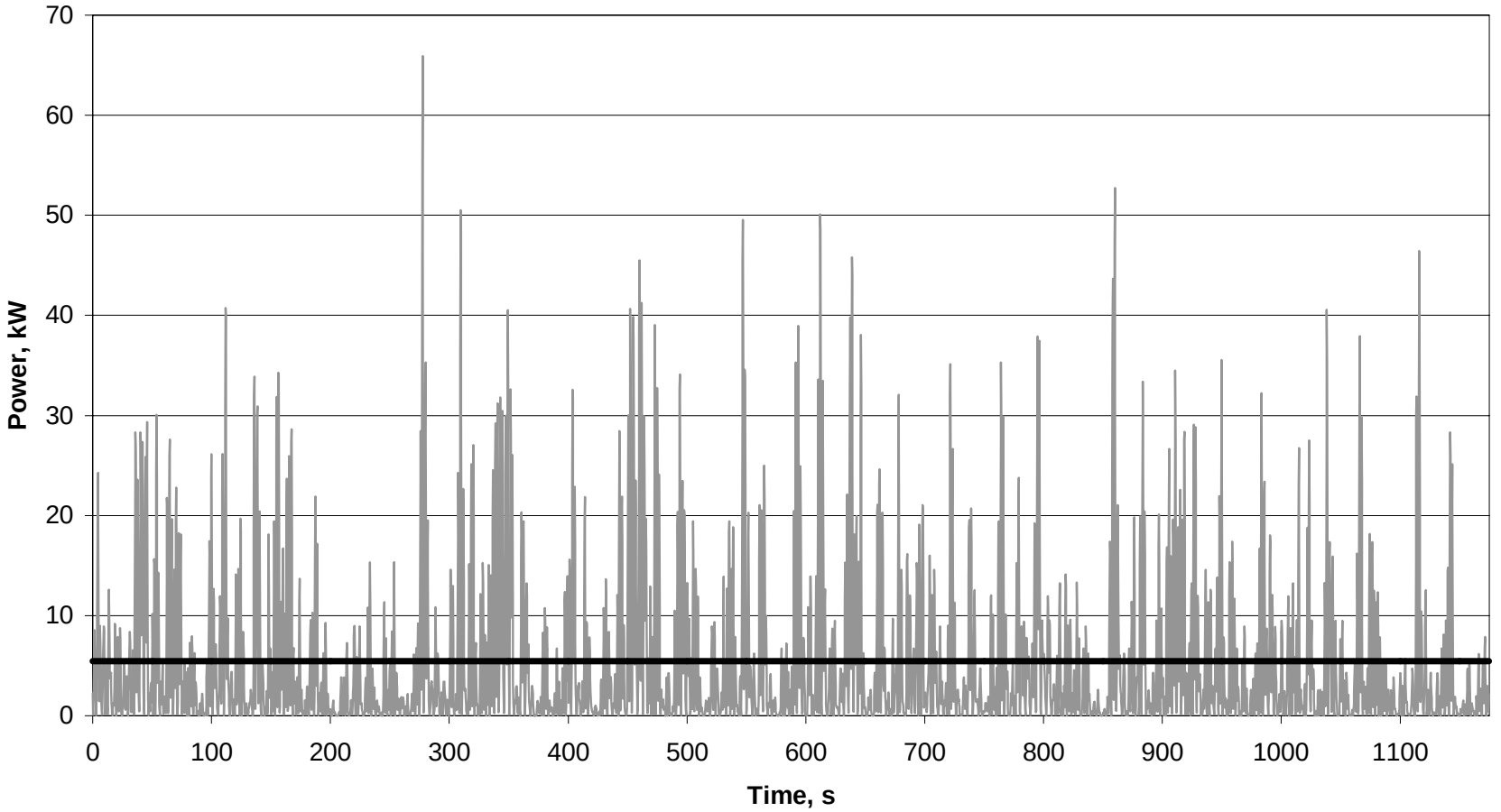
Total isentropic power generation. 1200, 18th January 2002
Power, kW
70
60
50
40
30
20
10
0
0
100
200
300
400
500
600
700
800
900
1000
1100
Time, s

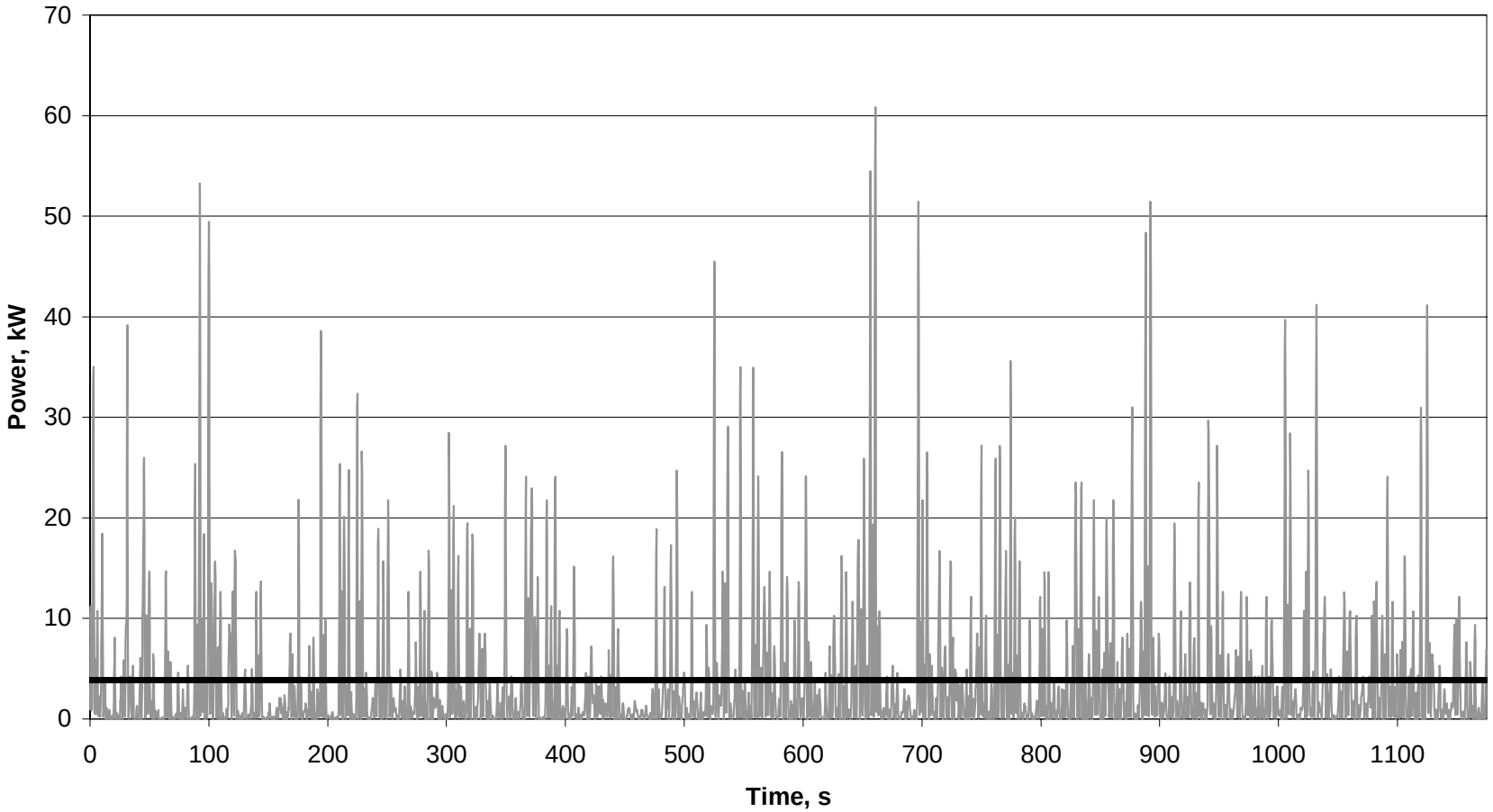
Isentropic power generation within column 1. 1200, 23rd January 2002
Power, kW
Time, s
0
10
20
30
40
50
60
70
0
100
200
300
400
500
600
700
800
900
1000
1100

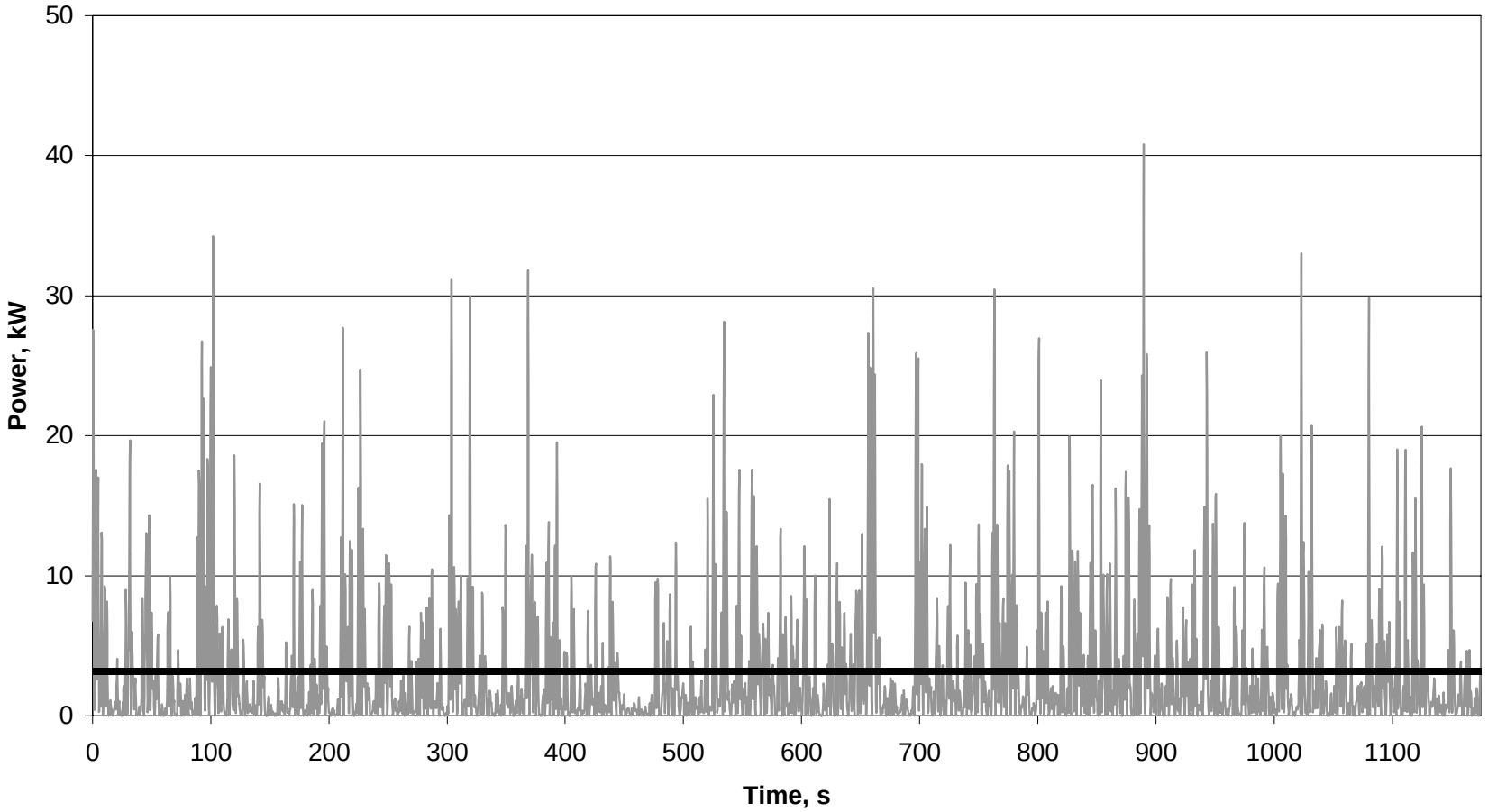
Isentropic power generation within column 2, 23rd January 2002
Power, kW
50
40
30
20
10
0
0
100
200
300
400
500
600
700
800
900
1000
1100
Time, s

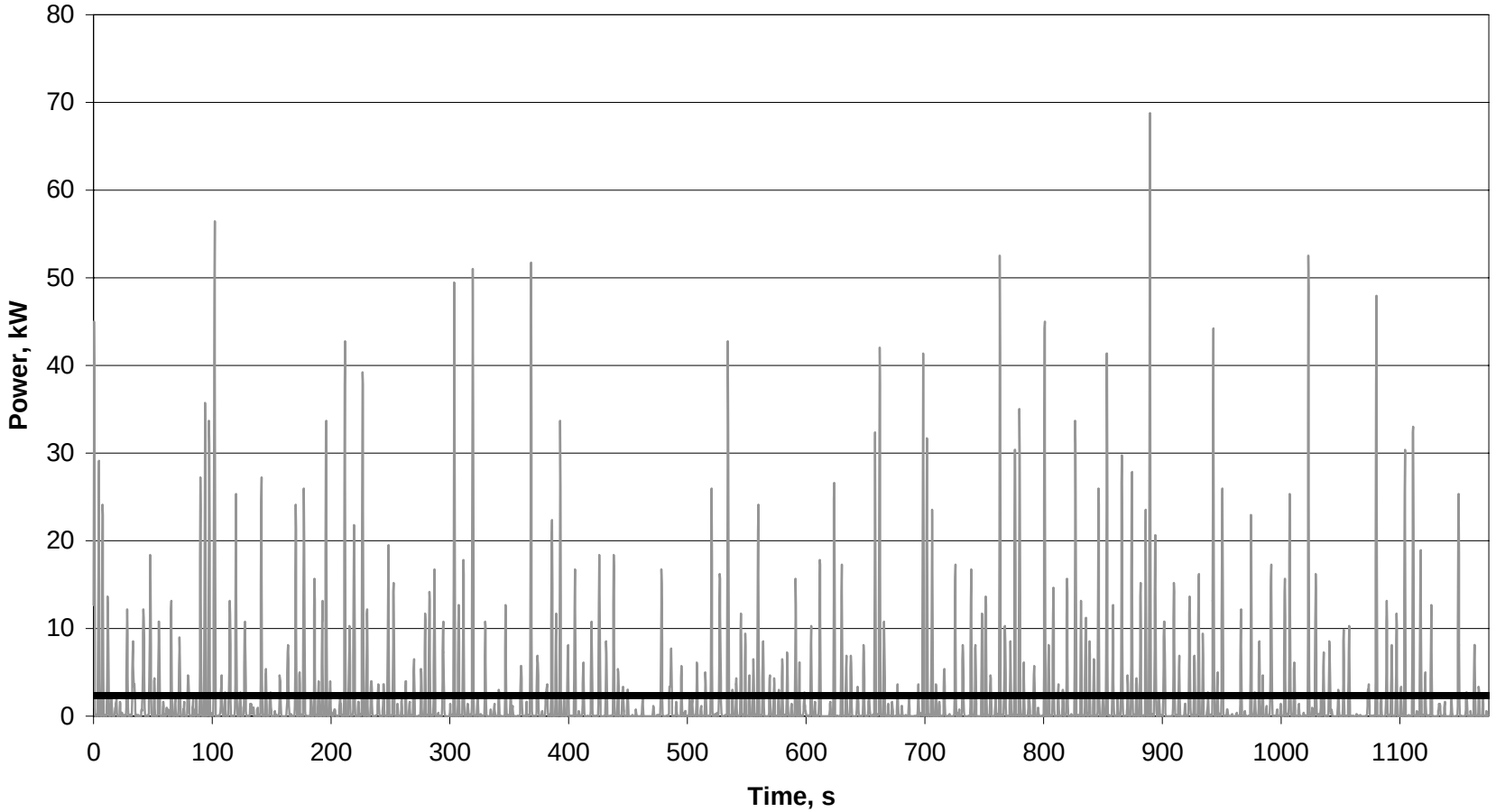
Isentropic power generation within column 3, 23rd January 2002
Power, kW
0
10
20
30
40
50
60
70
80
0
100
200
300
400
500
600
700
800
900
1000
1100
Time, s

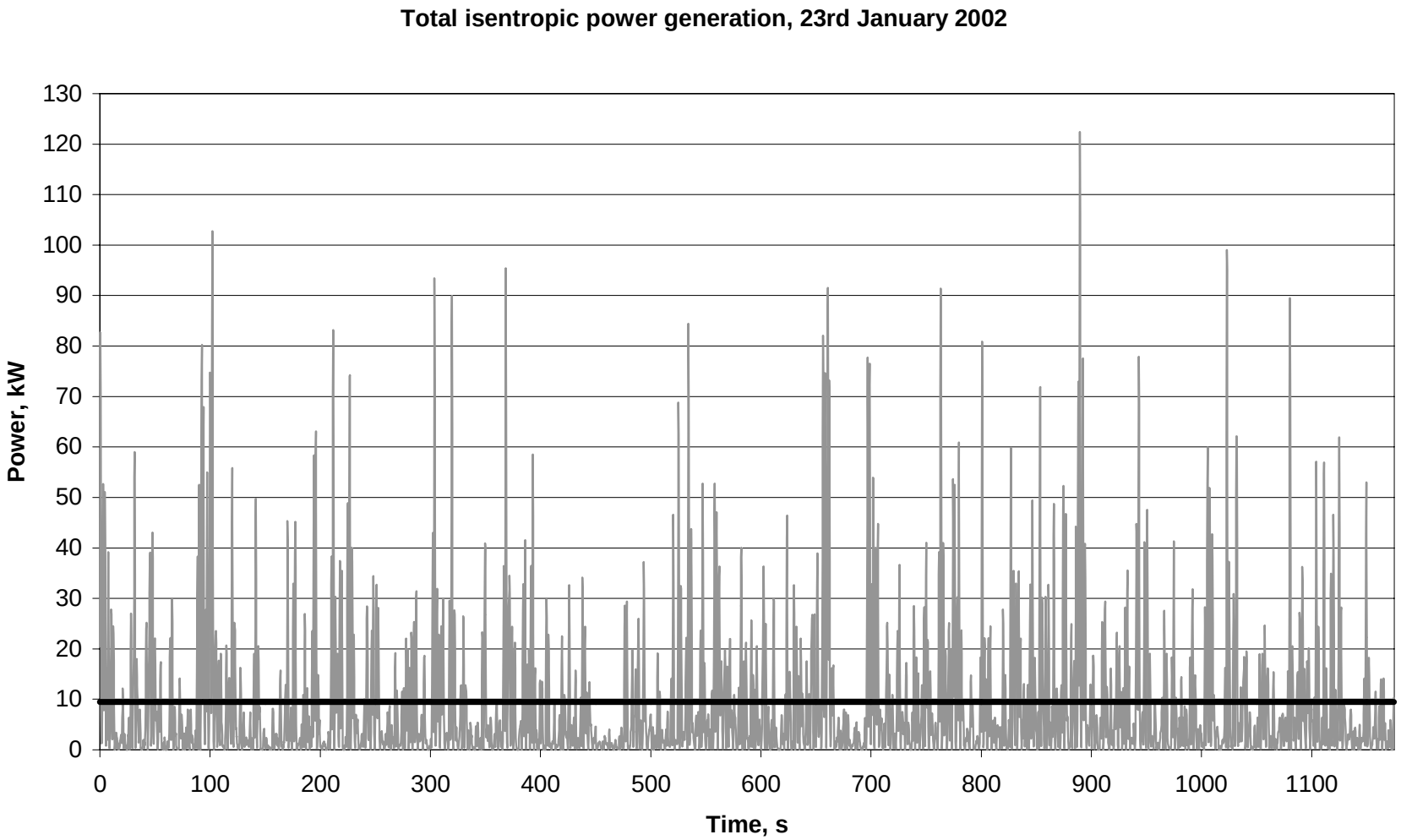
Total isentropic power generation, 23rd January 2002
Power, kW
130
120
110
100
90
80
70
60
50
40
30
20
10
0
0
100
200
300
400
500
600
700
800
900
1000
1100
Time, s